Electronic Supporting Information

for

# Azidophenyl as a click-transformable redox label of DNA suitable for electrochemical footprinting of DNA-protein interactions

**Jana Balintová,[a] Jan Špaček,[b] Radek Pohl,[a] Marie Brázdová,[b] Luděk Havran,[b,c] Miroslav Fojta*[b,c] and Michal Hocek*[a,d]**

[a] *Institute of Organic Chemistry and Biochemistry, Academy of Sciences of the Czech Republic, Gilead & IOCB Research Center, Flemingovo nam. 2, CZ-16610 Prague 6, Czech Republic; E-mail: hocek@uochb.cas.cz.*
[b] *Institute of Biophsics, v.v.i. Academy of Sciences of the Czech Republic; Kralovopolska 135, 61265 Brno, Czech Republic; E-mail: fojta@ibp.cz.*
[c] *Central European Institute of Technology, Masaryk University Kamenice 753/5, CZ-625 00 Brno, Czech Republic*
[d] *Department of Organic and Nuclear Chemistry, Faculty of Science, Charles University in Prague, Hlavova 8, CZ-12843 Prague 2, Czech Republic.*

Table of contents:

# 1 Single incorporation of functionalized dNTPs

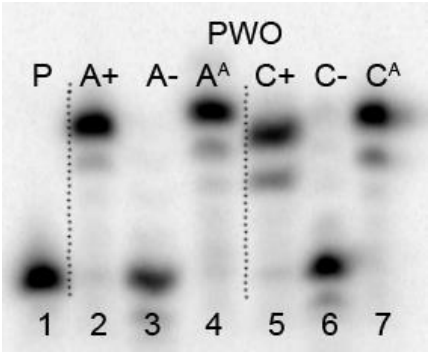


**Figure S1.** PEX single incorporations of a **dN$^{A}$TP** into 19-nt DNA using temp$^{C}$ or temp$^{A}$ template and PWO DNA polymerase.

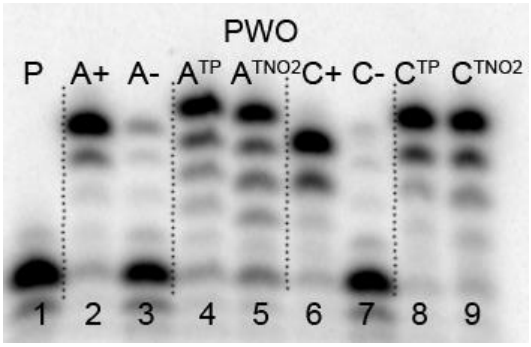


**Figure S2.** PEX single incorporations of a **dN$^{TP}$TP** and **dN$^{TNO2}$TP** into 19-nt DNA using temp$^{C}$ or temp$^{A}$ template and Pwo DNA polymerase.

# 2 Kinetics study

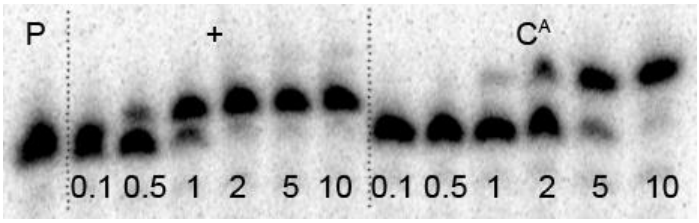


**Figure S3.** Kinetics of PEX using **dC$^{A}$TP** in comparison with natural **dCTP** (+). Time intervals are given in minutes.

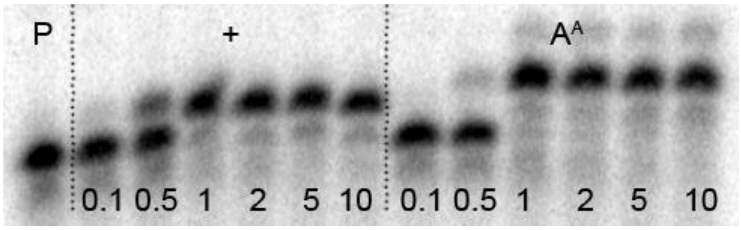


**Figure S4.** Kinetics of PEX using **dA$^{A}$TP** in comparison with natural **dATP** (+). Time intervals are given in minutes.

# 3 Multiple incorporations of functionalized dNTPs

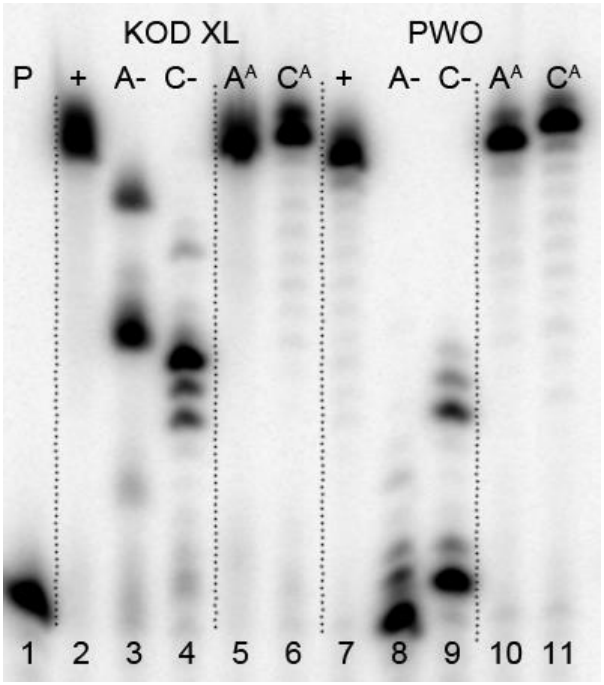


**Figure S5.** PEX incorporations of a **dN$^{A}$TP** into 31-nt DNA using temp$^{rnd16}$ template, KOD XL and PWO DNA polymerase.

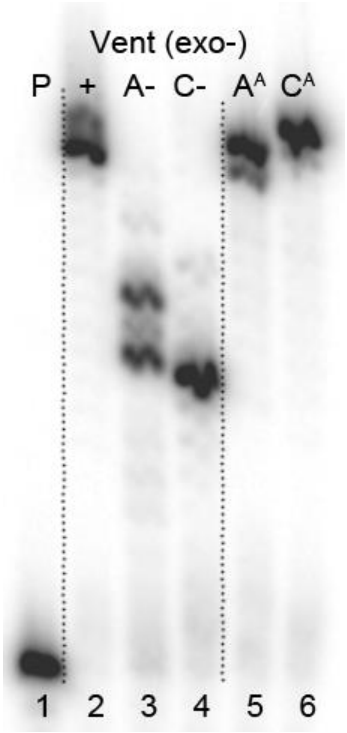


**Figure S6.** PEX incorporations of a **dN$^{A}$TP** into 31-nt DNA using temp$^{rnd16}$ template, Vent (*exo-)* DNA polymerase.

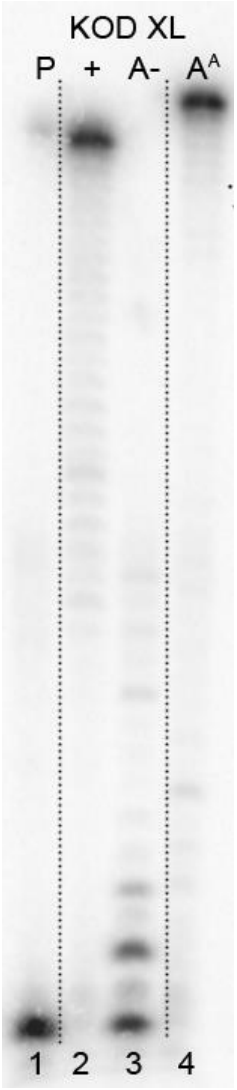


**Figure S7.** PEX incorporations of a **dN$^{A}$TP** into 50-nt DNA using template temp$^{2CON4}$ and KOD XL DNA polymerase.

# 4 Study of DNA-protein interaction

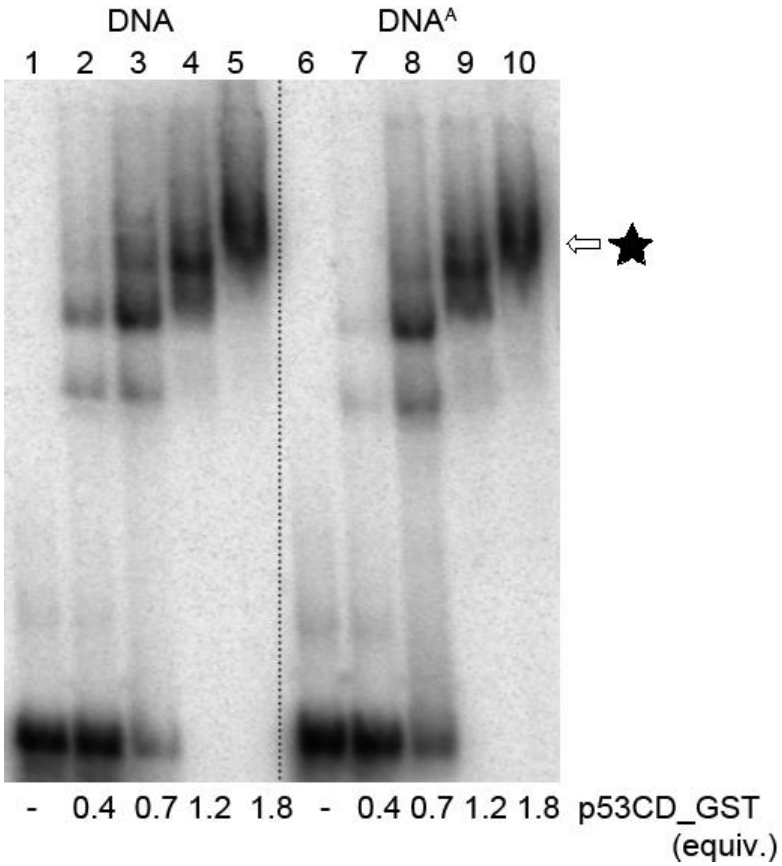


**Figure S8. Native PAGE analysis of 50-mer DNA$^{2CON4}$_p53CD_GST complex.** Lane 1: natural DNA; 2: 0.4 equiv.; 3: 0.7 equiv.; 4: 1.2 equiv.; 5: 1.8 equiv. of protein p53CD_GST to DNA; Lane 6: DNA$^{A}$; 7: 0.4 equiv.; 8: 0.7 equiv.; 9: 1.2 equiv.; 10: 1.8 equiv. of protein p53CD_GST to DNA.


**Figure S9. Native PAGE analysis of stability of DNA$^{2CON4}$_p53CD_GST complex after click reaction.** Lane 1: DNA$^{A}$; lane 2: protein/DNAcomplex; lane 3: protein/DNAcomplex, 0.5 mM 4-nitrophenylacetylene, 5 μM CuBr; 25 μM TBTA ligand, 65 μM Na ascorbate, 20 ºC, 1h.

# 5 Thermal stability of complex DNA-protein

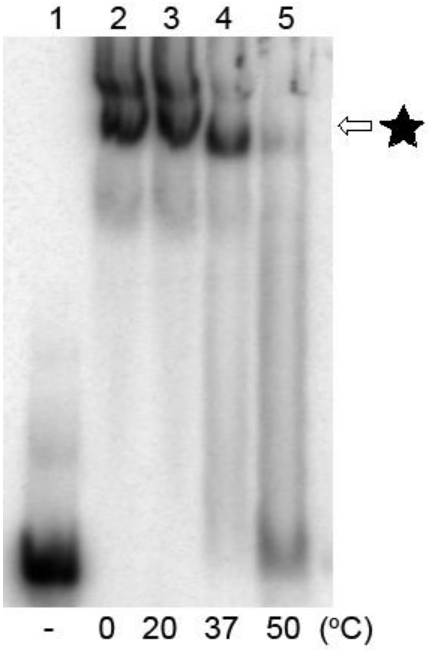


**Figure S10. Native PAGE analysis of thermal stability of DNA$^{1a2G}$_p53CD_GST complex.** Lane 1: DNA$^{A}$; lanes 2-5: 1.2 equiv. of protein p53CD_GST to DNA. **Conditions:** DNA and proteins were mixed together in binding buffer and created protein/DNA complexes were incubated at mentioned temperatures for 1h.

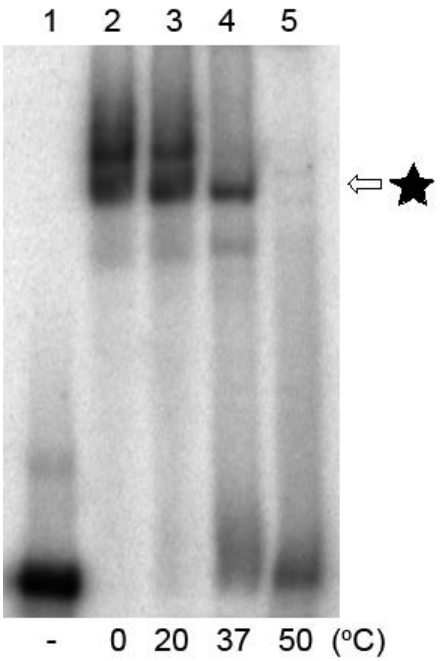


**Figure S11. Native PAGE analysis of thermal stability of DNA$^{2CON4}$_p53CD_GST complex.** Lane 1: DNA$^{A}$; lanes 2-5: 1.2 equiv. of protein p53CD_GST to DNA. **Conditions:** DNA and proteins were mixed together in binding buffer and created protein/DNA complexes were incubated at mentioned temperatures for 1h.

# 6 $Cu^{I}$ concentration dependence of stability of complex DNA-protein

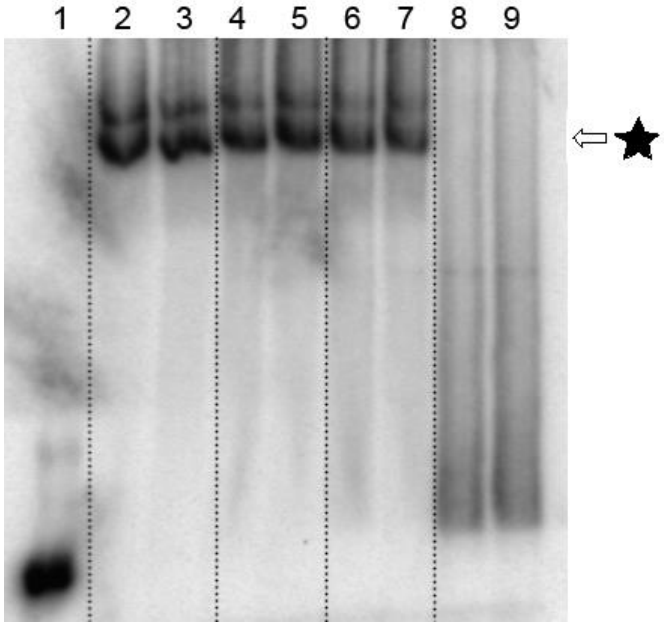


**Figure S12. Native PAGE analysis of $Cu^{I}$ concentration dependence of stability of $DNA^{1a2G}$_p53CD_GST complex.** Lane 1: $DNA^{A}$; lanes 2-9: 1.2 equiv. of protein p53CD_GST to DNA; lane 2: protein/DNAcomplex; lane 3: protein/DNAcomplex, 20ºC; lane 4: protein/DNAcomplex, 5 μM CuBr, 20ºC; lane 5: protein/DNAcomplex, 5 μM CuBr, 25 μM TBTA ligand, 20ºC; lane 6: protein/DNAcomplex, 10 μM CuBr, 20ºC; lane 7: protein/DNAcomplex, 10 μM CuBr; 50 μM TBTA ligand, 20ºC; lane 8: protein/DNAcomplex, 20 μM CuBr, 20ºC; lane 9: protein/DNAcomplex, 20 μM CuBr; 100 μM TBTA ligand, 20ºC. **Conditions:** DNA and proteins were mixed together in binding buffer and created protein/DNAcomplexes were incubated with various concentration of CuBr in/without presence of the TBTA ligand at 20ºC for 1h.

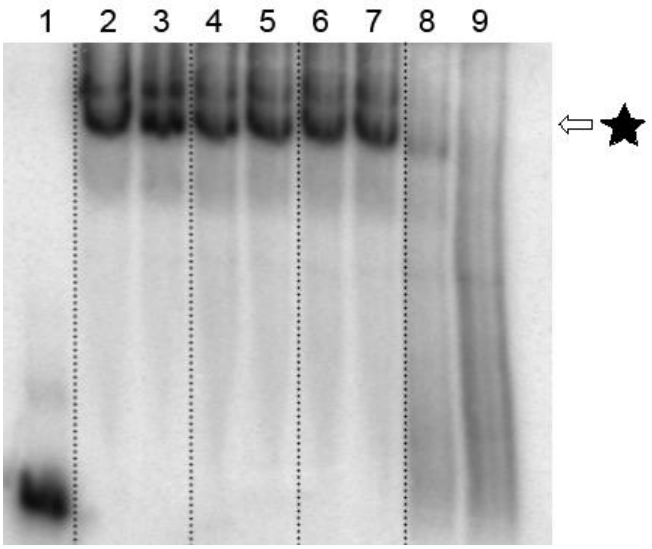


**Figure S13. Native PAGE analysis of $Cu^{I}$ concentration dependence of stability of $DNA^{2CON4}$_p53CD_GST complex.** Lane 1: $DNA^{A}$; lanes 2-9: 1.2 equiv. of protein p53CD_GST to DNA; lane 2: protein/DNAcomplex; lane 3: protein/DNAcomplex, 20ºC; lane 4: protein/DNAcomplex, 5µ M CuBr, 20ºC; lane 5: protein/DNAcomplex, 5 µM CuBr, 25 µM TBTA ligand, 20ºC; lane 6: protein/DNAcomplex, 10 µM CuBr, 20ºC; lane 7: protein/DNAcomplex, 10 µM CuBr; 50 µM TBTA ligand, 20ºC; lane 8: protein/DNAcomplex, 20 µM CuBr, 20ºC; lane 9: protein/DNAcomplex, 20 µM CuBr; 100 µM TBTA ligand, 20ºC. **Conditions:** DNA and proteins were mixed together in binding buffer and created protein/DNAcomplexes were incubated with various concentration of CuBr in/without presence of the TBTA ligand at 20ºC for 1h.

# 7 Electrochemistry

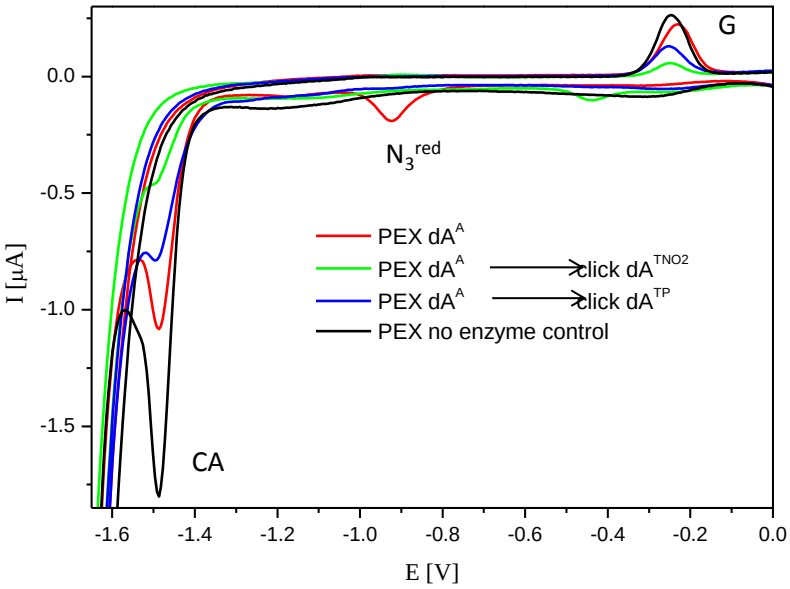


**Figure S14.** CV responses at HMDE of PEX products synthesized with temp$^{rnd16}$ template and dNTP mixes containing **dA$^{A}$TP** (as specified in legend) complemented with three natural dNTPs and PEX products after click reaction with (nitro)phenyltriazole. CA – peak due to reduction of cytosine and adenine, G – peak due to guanine, $N_3^{red}$ – azide reduction, $NO_2^{red}$ – nitrogroup reduction.

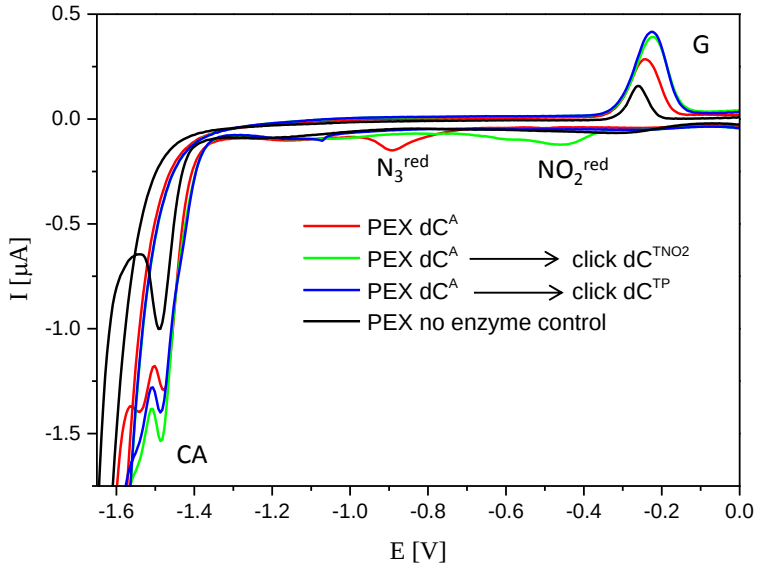


**Figure S15.** CV responses at HMDE of PEX products synthesized with temp$^{rnd16}$ template and dNTP mixes containing **dC$^{A}$TP** (as specified in legend) complemented with three natural dNTPs and PEX products after click reaction with (nitro)phenyltriazole.

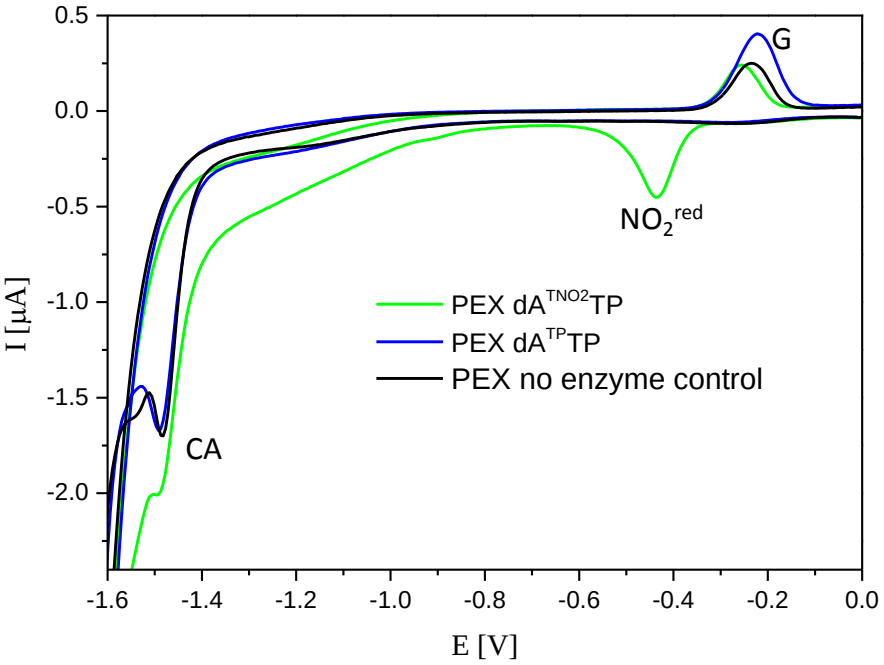


**Figure S16.** CV responses at HMDE of PEX products synthesized with temp$^{rnd16}$ template and dNTP mixes containing **dA$^{TX}$TP** (as specified in legend) complemented with three natural dNTPs.

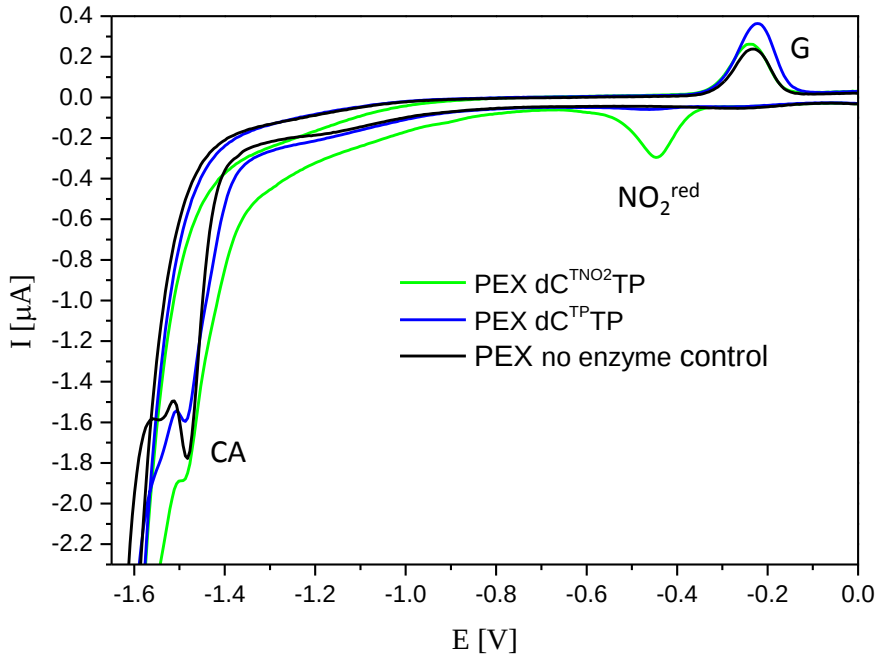


**Figure S17.** CV responses at HMDE of PEX products synthesized with temp$^{rnd16}$ template and dNTP mixes containing **dC$^{TX}$TP** (as specified in legend) complemented with three natural dNTPs.

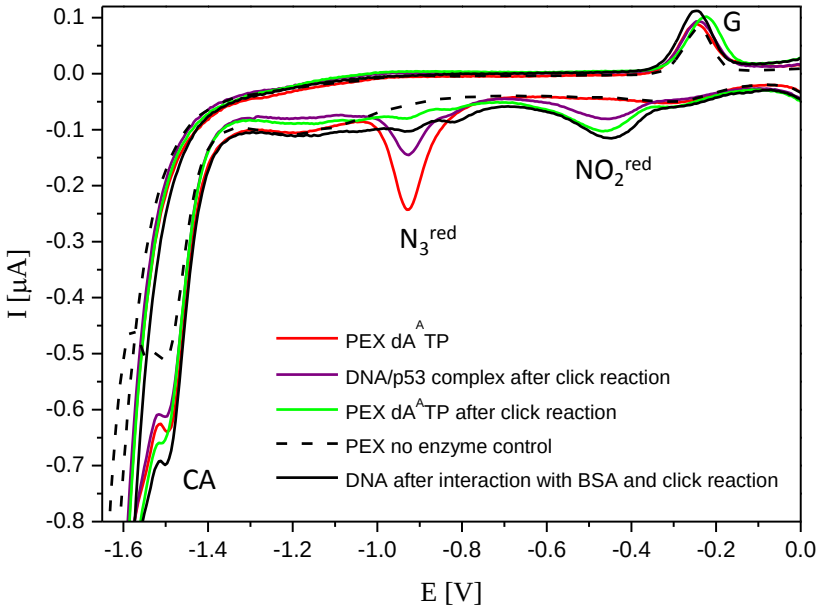


**Figure S18.** CV responses at HMDE of PEX products synthesized with temp$^{1a2G}$ template and **dA$^A$TP** complemented with three natural dNTPs (red curve) and PEX products after click reaction with nitrophenylacetylene (green curve), DNA-p53 complex after click reaction followed by denaturation (violet curve), control with BSA (black curve).

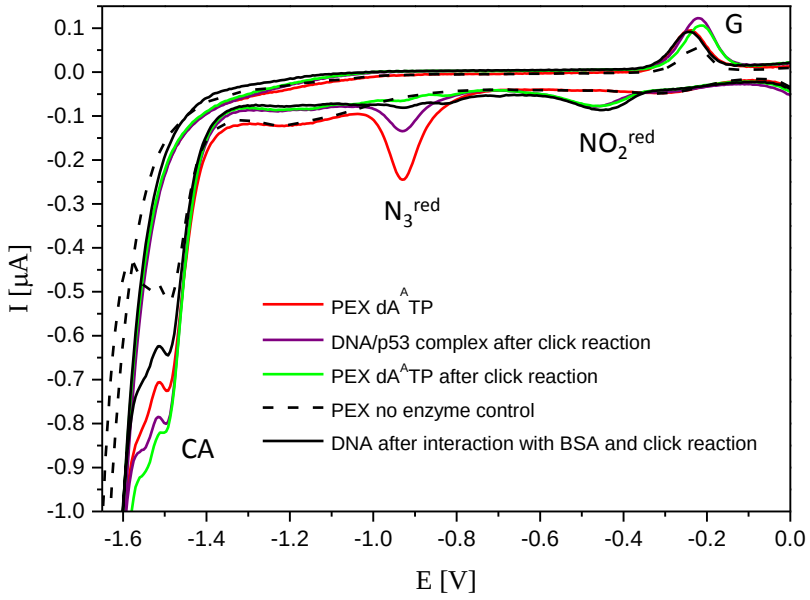


**Figure S19.** CV responses at HMDE of PEX products synthesized with temp$^{2CON4}$ template and **dA$^A$TP** complemented with three natural dNTPs (red curve) and PEX products after click reaction with nitrophenylacetylene (green curve), DNA-protein complex after click reaction followed by denaturation (violet curve), control with BSA (black curve).

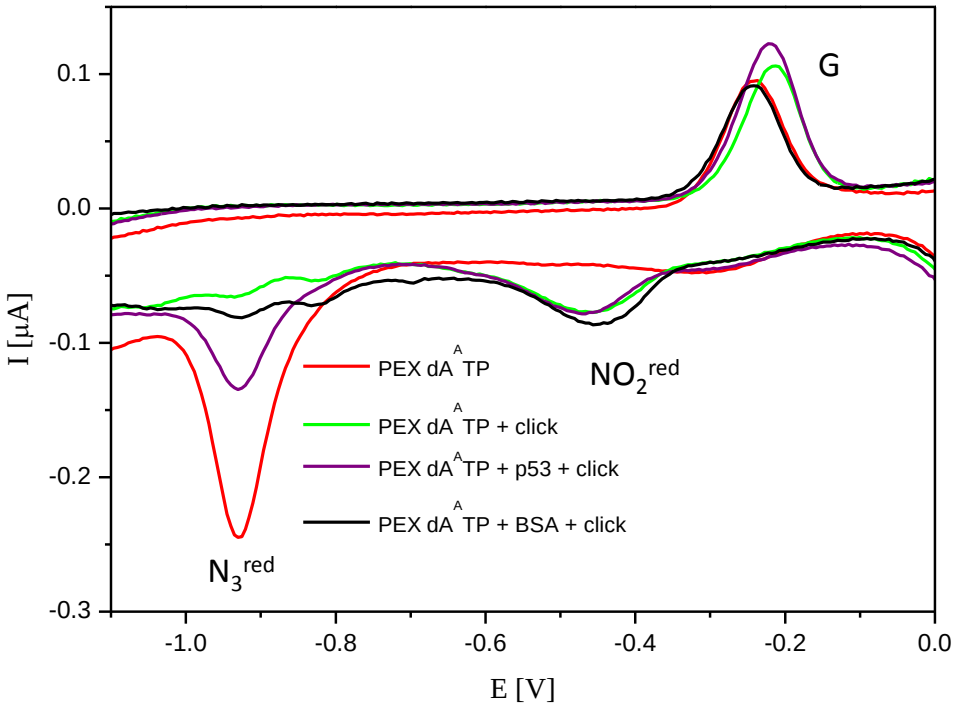


**Figure S20.** Detail of CV responses at HMDE of PEX products synthesized with temp$^{2CON4}$ template and **dA$^{A}$TP** complemented with three natural dNTPs (red curve) and PEX products after click reaction with nitrophenylacetylene (green curve), DNA-protein complex after click reaction followed by denaturation (violet curve), the control with BSA (black curve). For full CV scans see Fig. S19.

# 8 Selected copies of NMR spectra

$^{1}$H NMR and $^{13}$C spectra of **dC$^{A}$.**

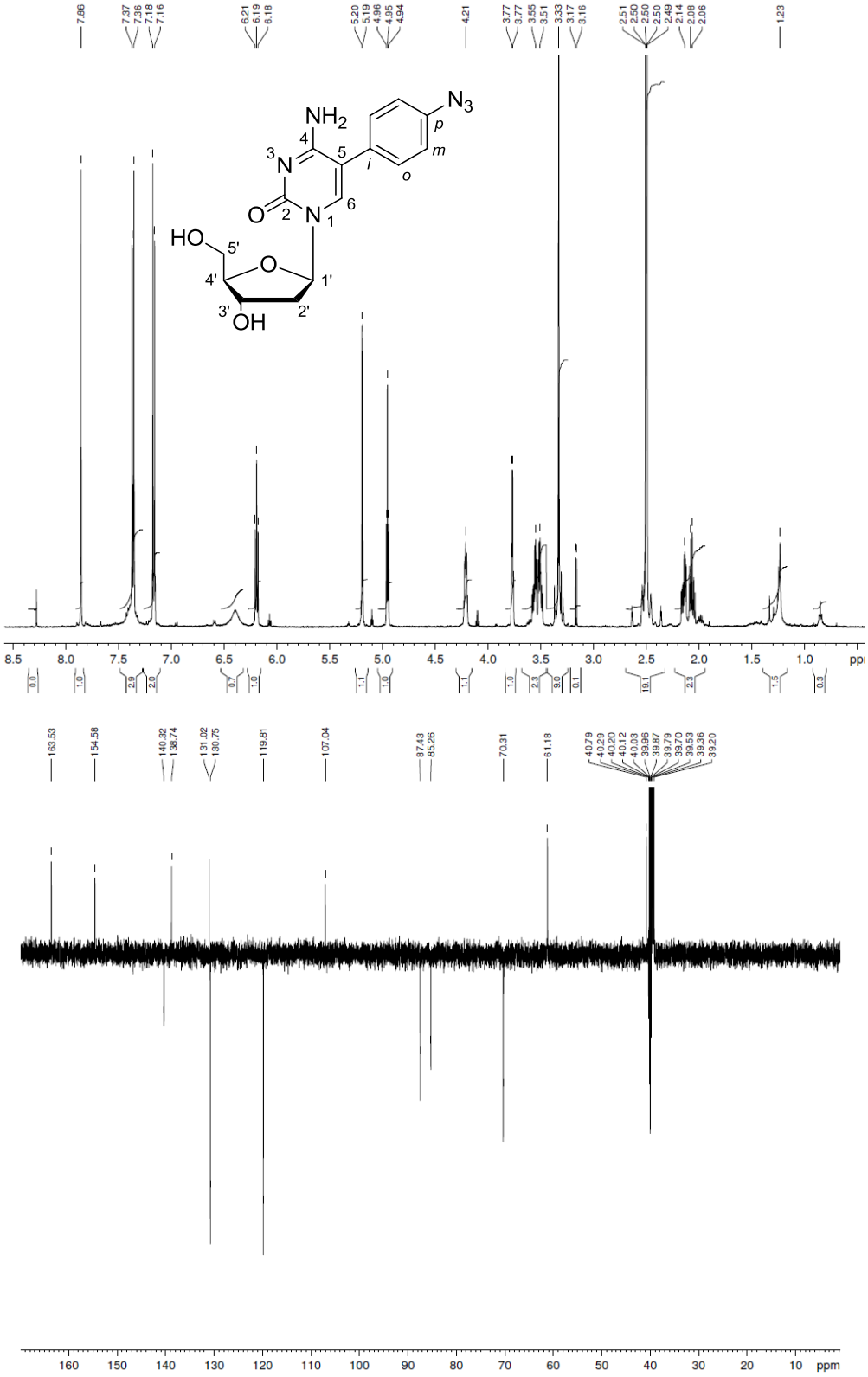

$^{1}$H NMR and $^{13}$C spectra of **dA$^{A}$.**

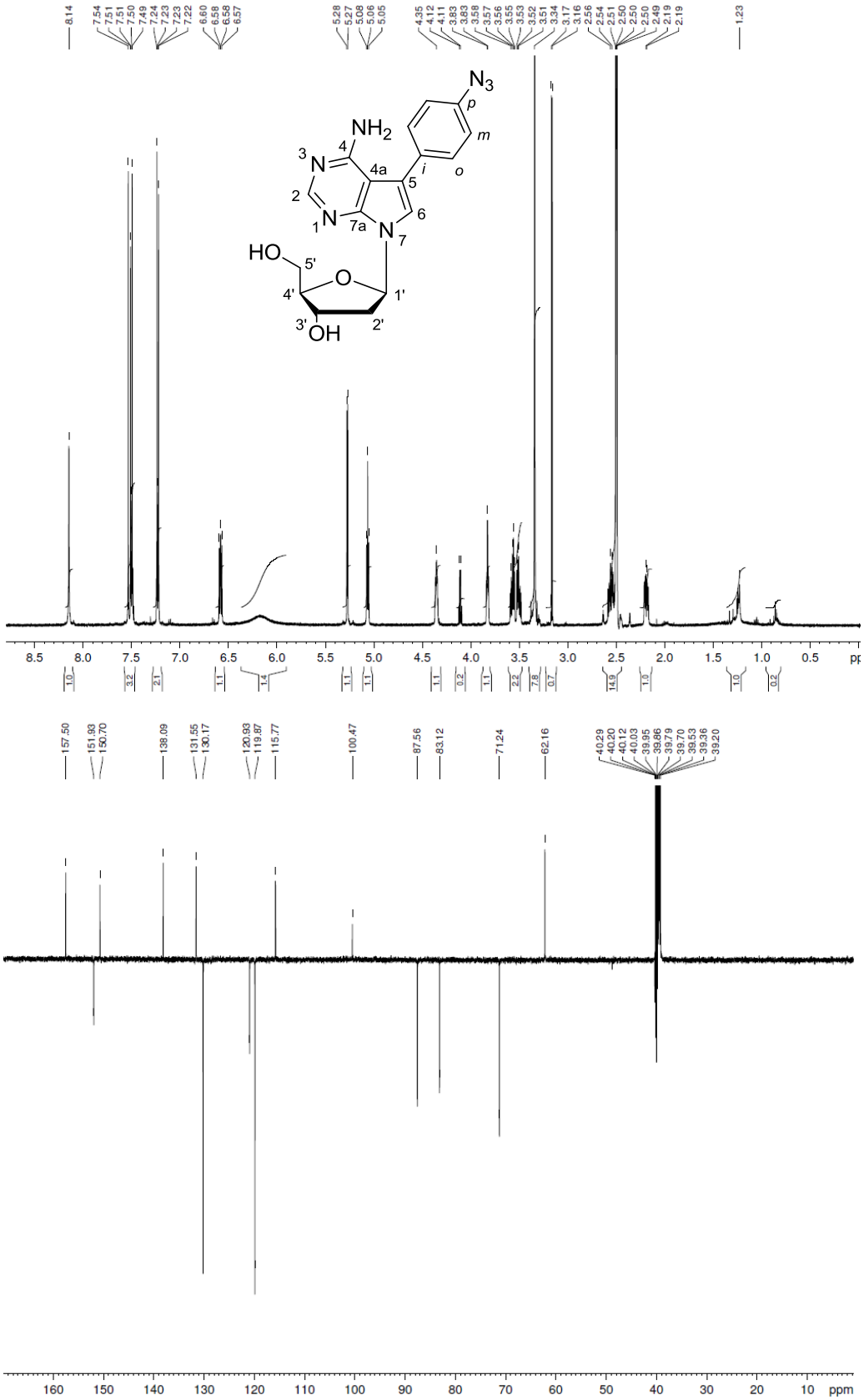

$^{1}$H NMR and $^{13}$C spectra of **dC$^{TP}$.**

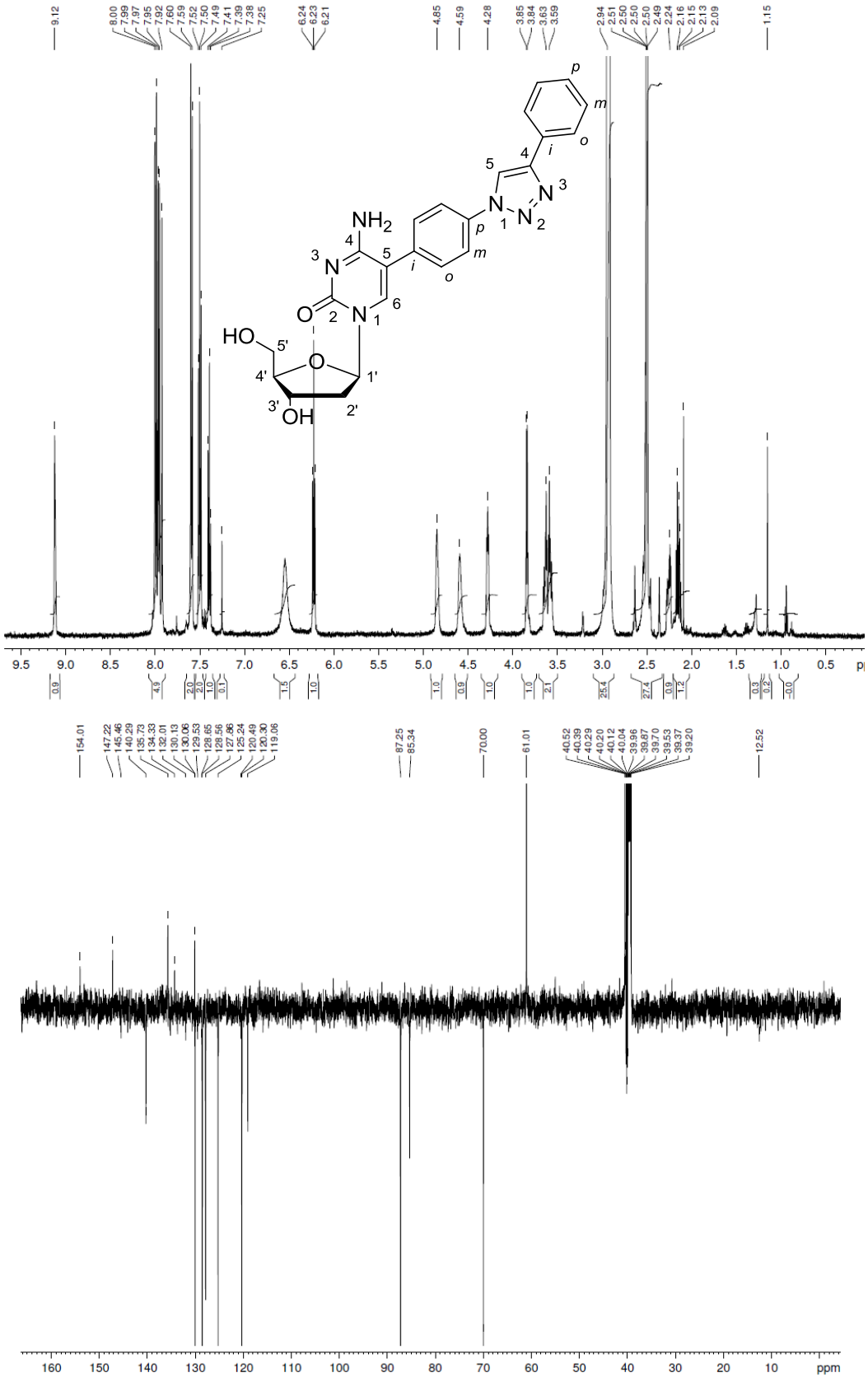

$^{1}$H NMR and $^{13}$C spectra of **dA$^{TP}$.**

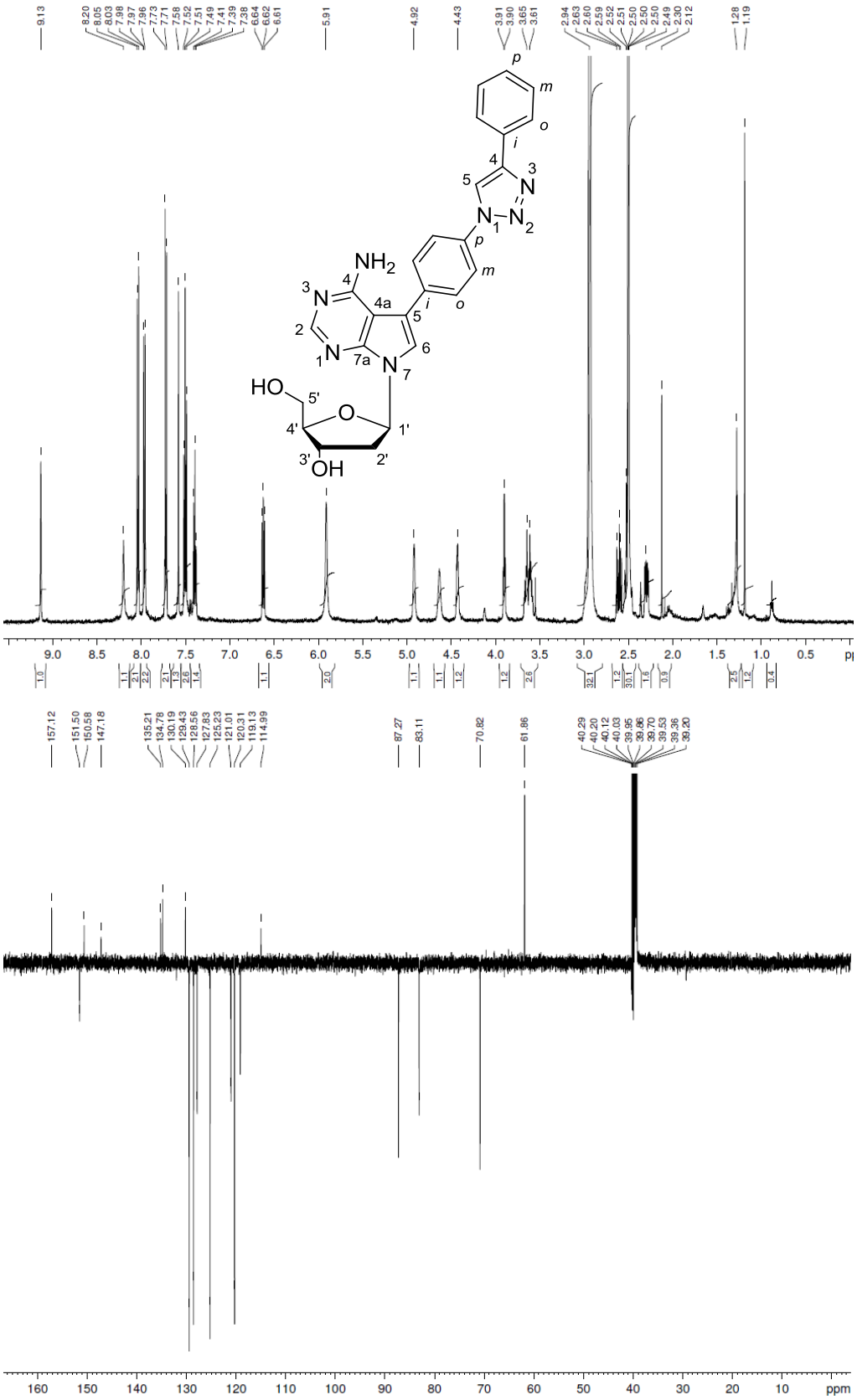

$^{1}$H NMR and $^{13}$C spectra of **dC$^{TNO2}$.**

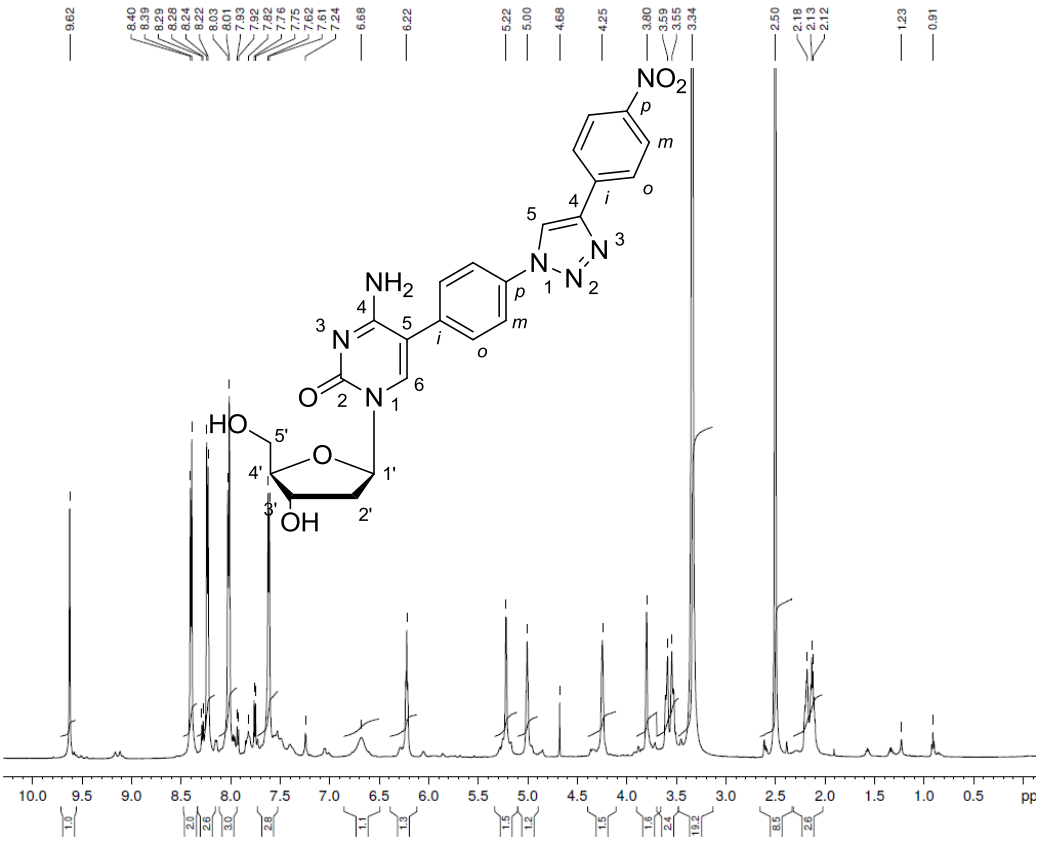


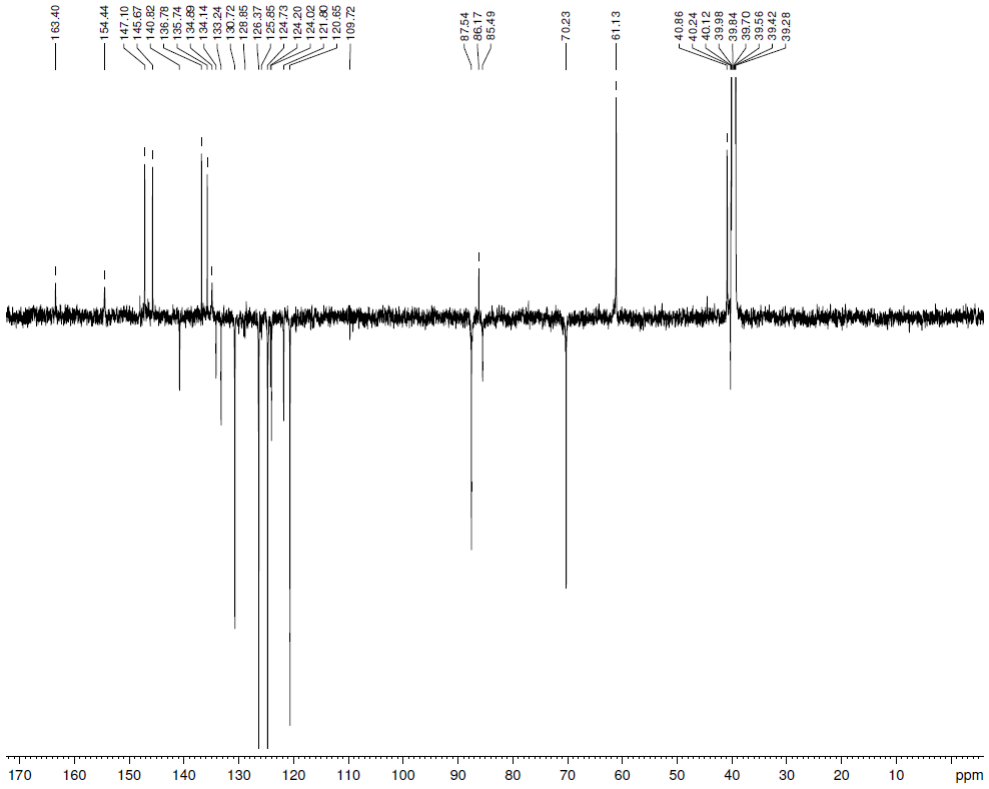

$^{1}$H NMR and $^{13}$C spectra of **dA$^{TNO2}$.**

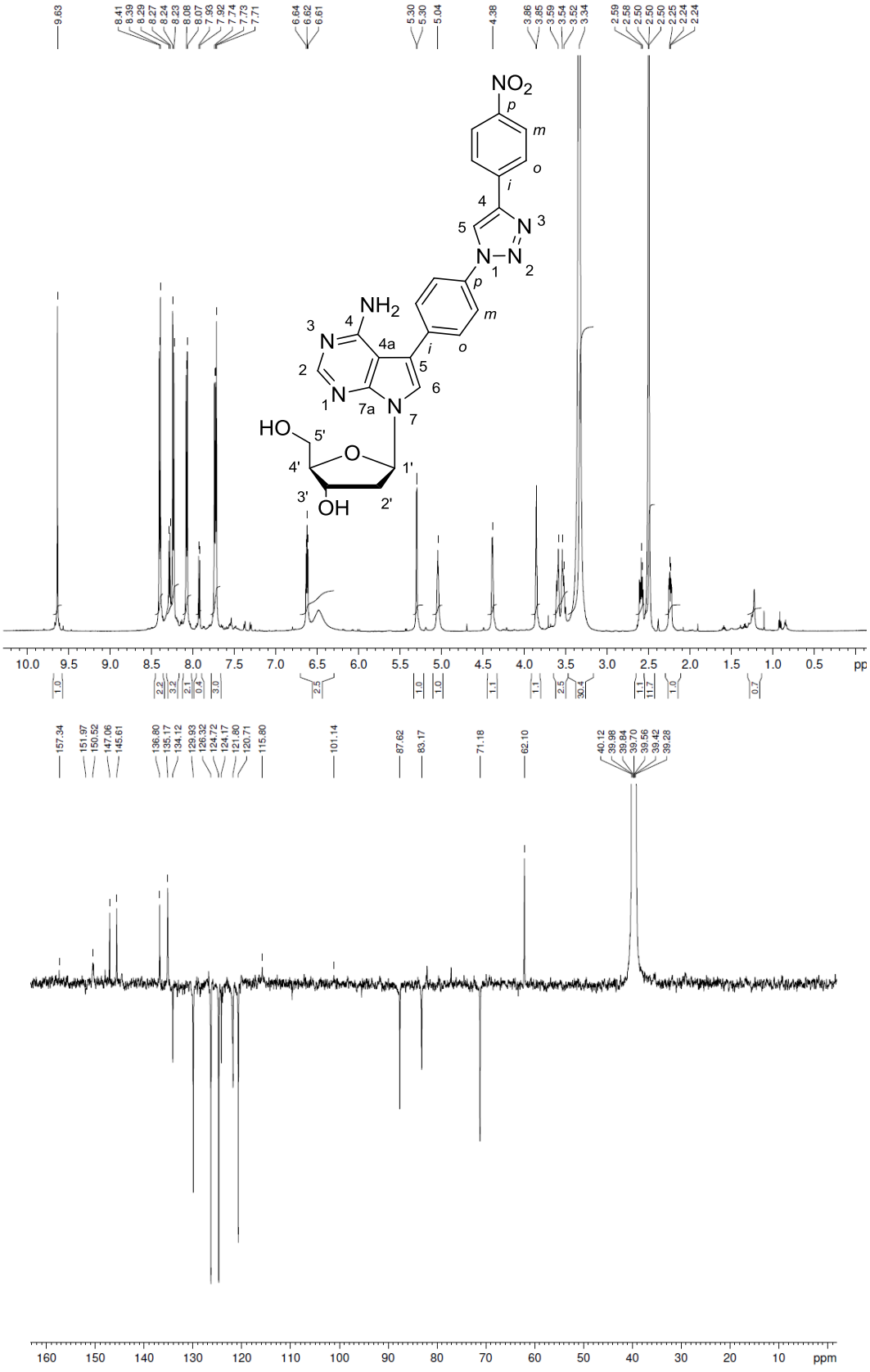

$^{1}$H NMR, $^{13}$C and $^{31}$P spectra of **dC$^{A}$TP.**

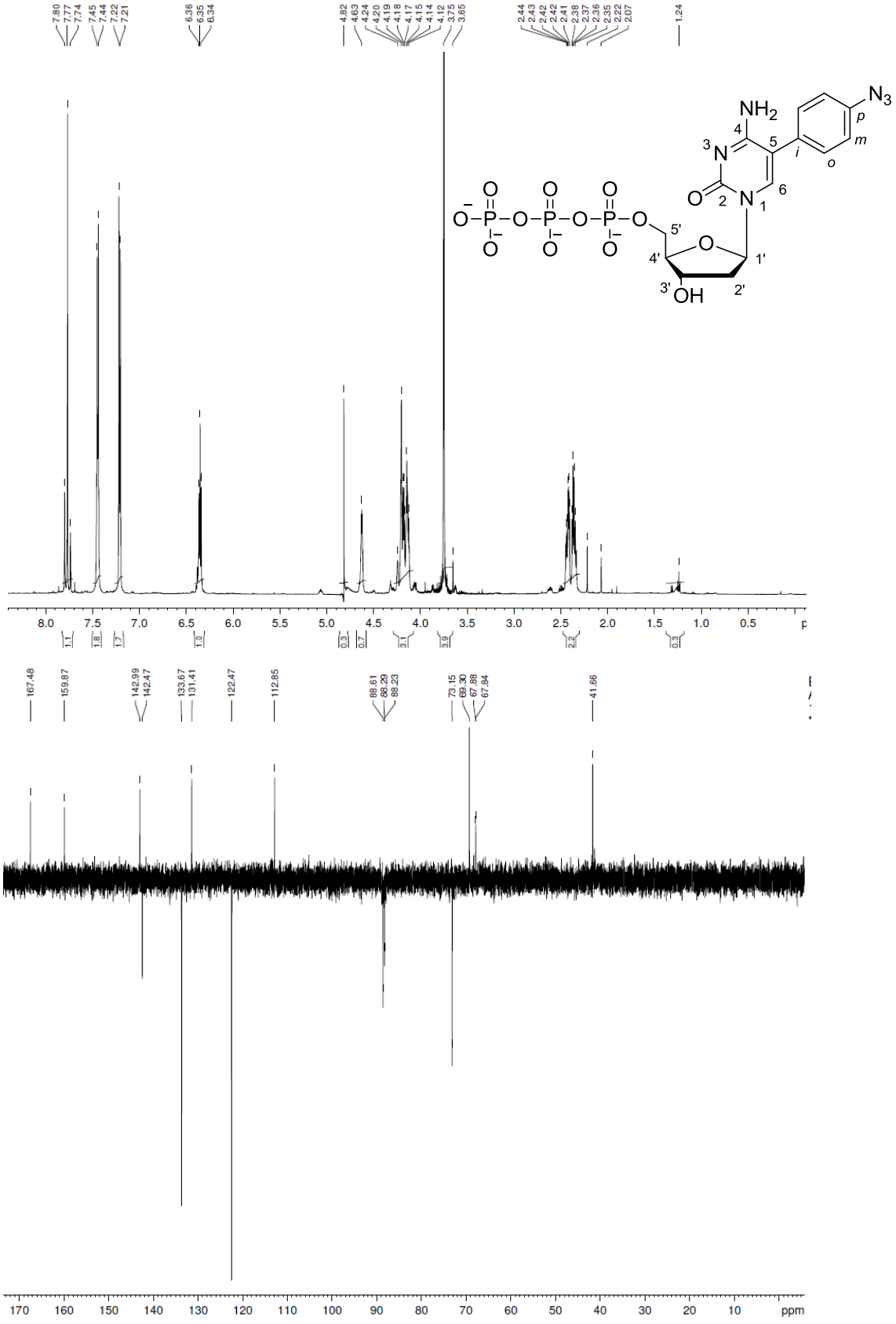

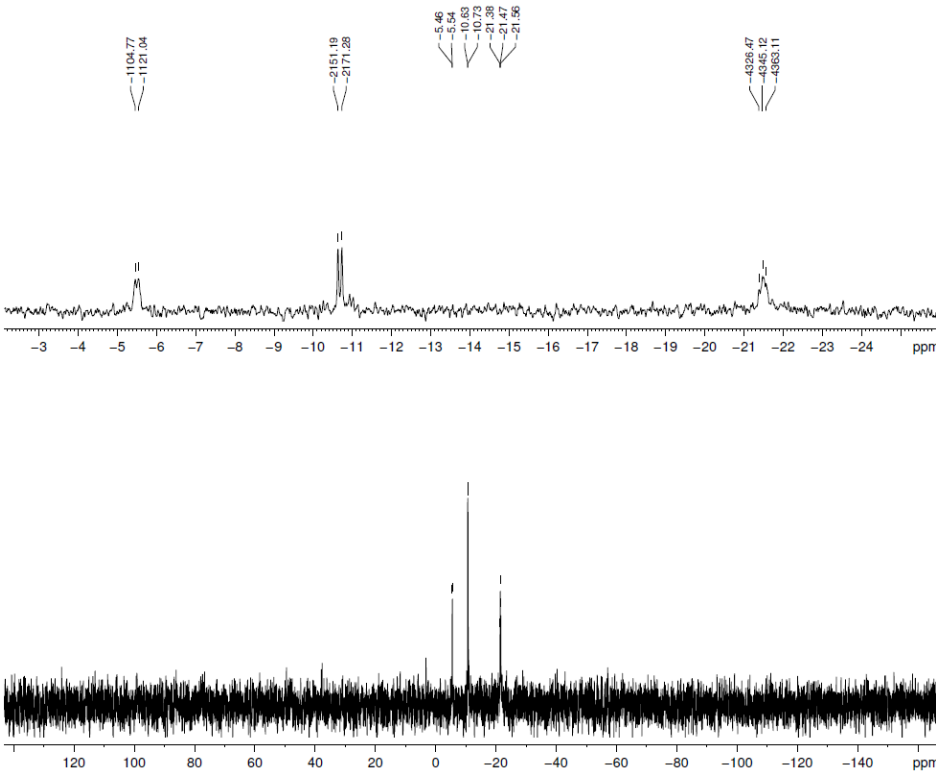

$^{1}$H NMR, $^{13}$C and $^{31}$P spectra of **dA$^{A}$TP.**

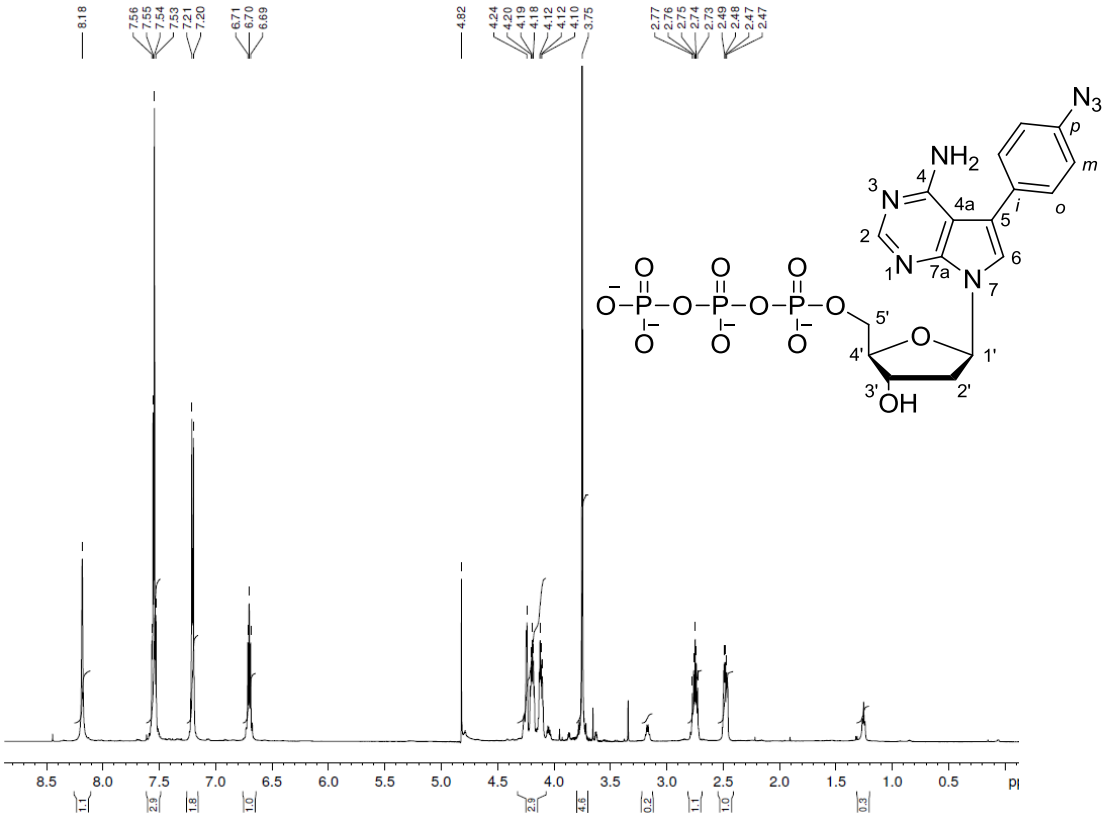

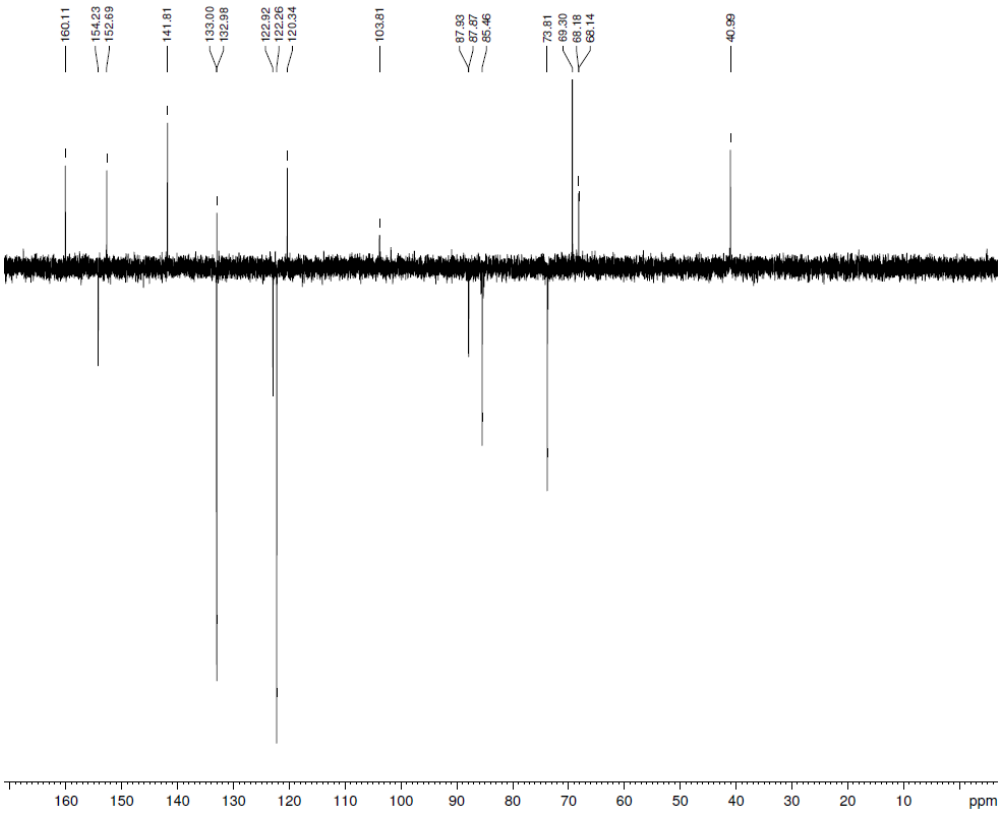
160.11
154.23
152.69
141.81
133.00
132.98
122.92
122.26
120.34
103.81
87.93
87.87
85.46
73.81
69.30
68.18
68.14
40.99
160 150 140 130 120 110 100 90 80 70 60 50 40 30 20 10 ppm

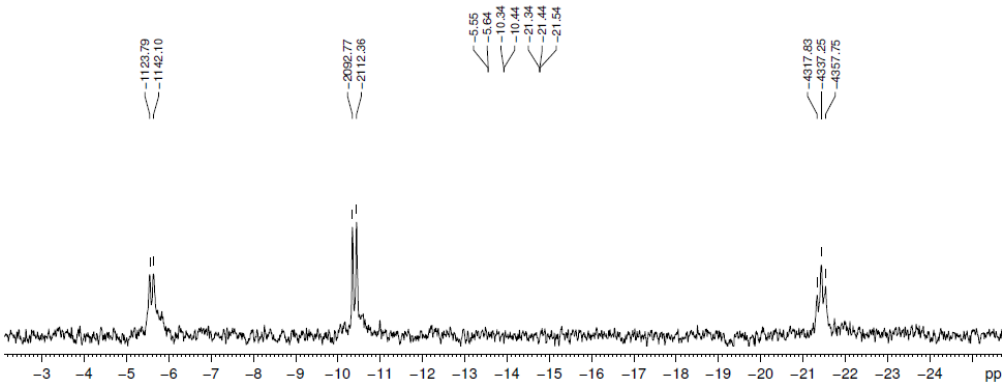
-1123.79
-1142.10
-2092.77
-2112.36
-5.55
-5.64
-10.34
-10.44
-21.34
-21.44
-21.54
-4317.83
-4337.25
-4357.75
−3 −4 −5 −6 −7 −8 −9 −10 −11 −12 −13 −14 −15 −16 −17 −18 −19 −20 −21 −22 −23 −24 pp

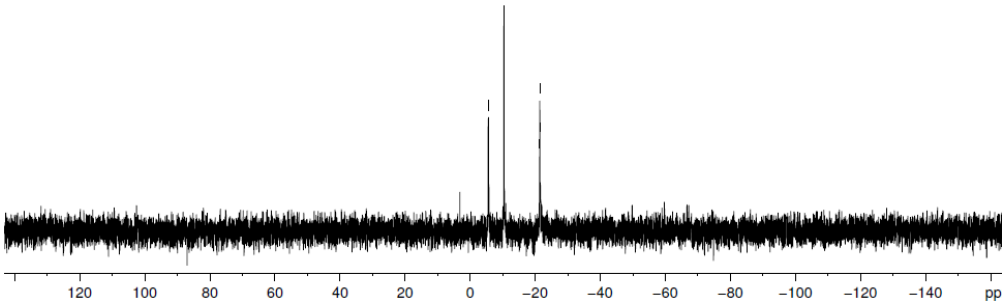
120 100 80 60 40 20 0 −20 −40 −60 −80 −100 −120 −140 pp

$^{1}$H NMR, $^{13}$C and $^{31}$P spectra of **dC$^{TP}$TP.**

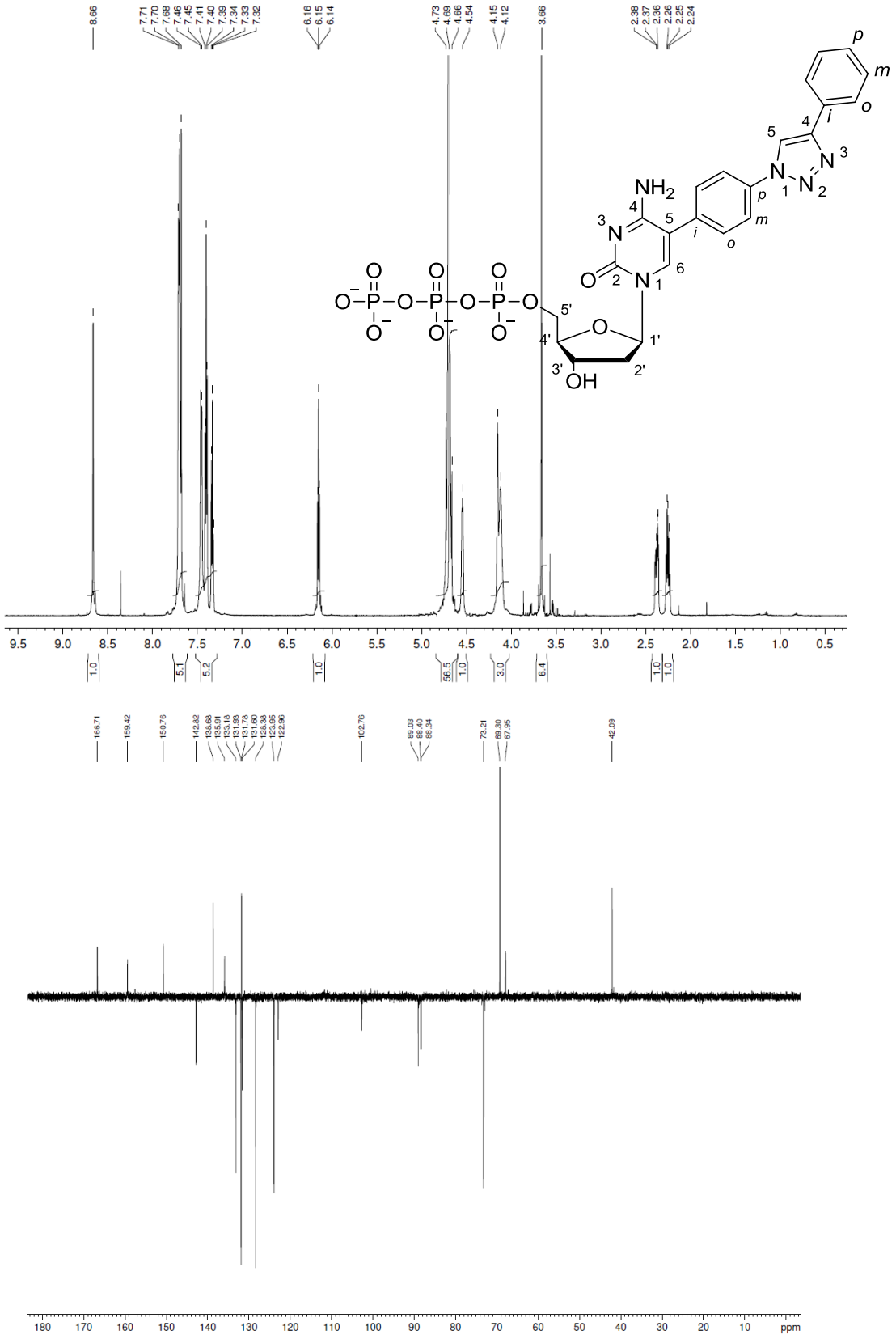

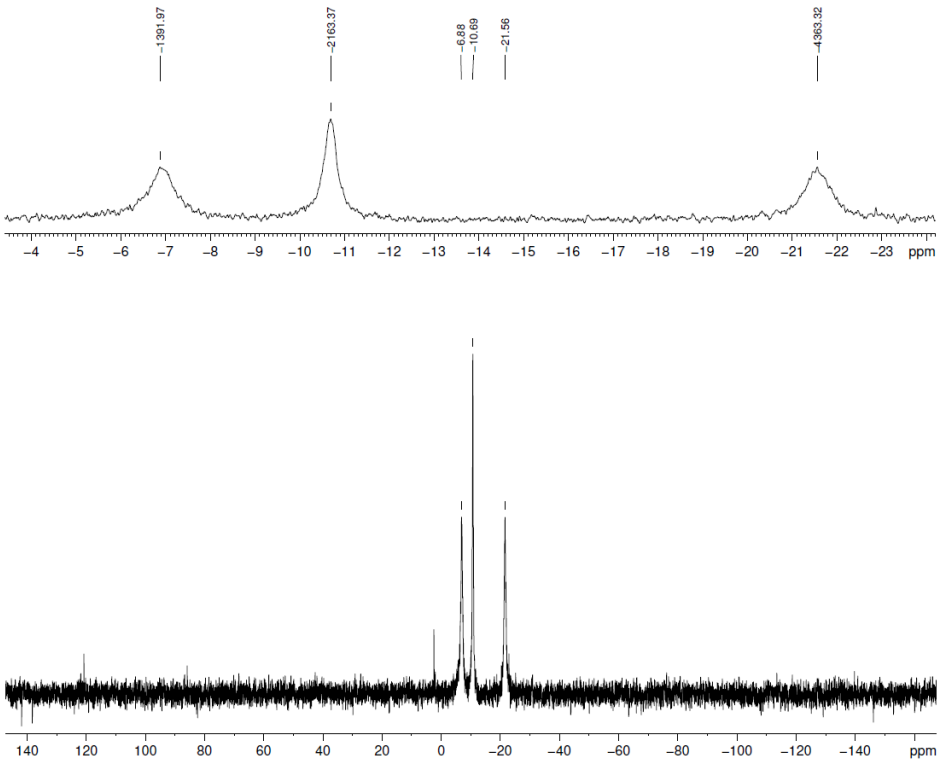


$^{1}$H NMR, $^{13}$C and $^{31}$P spectra of **dA$^{TP}$TP.**

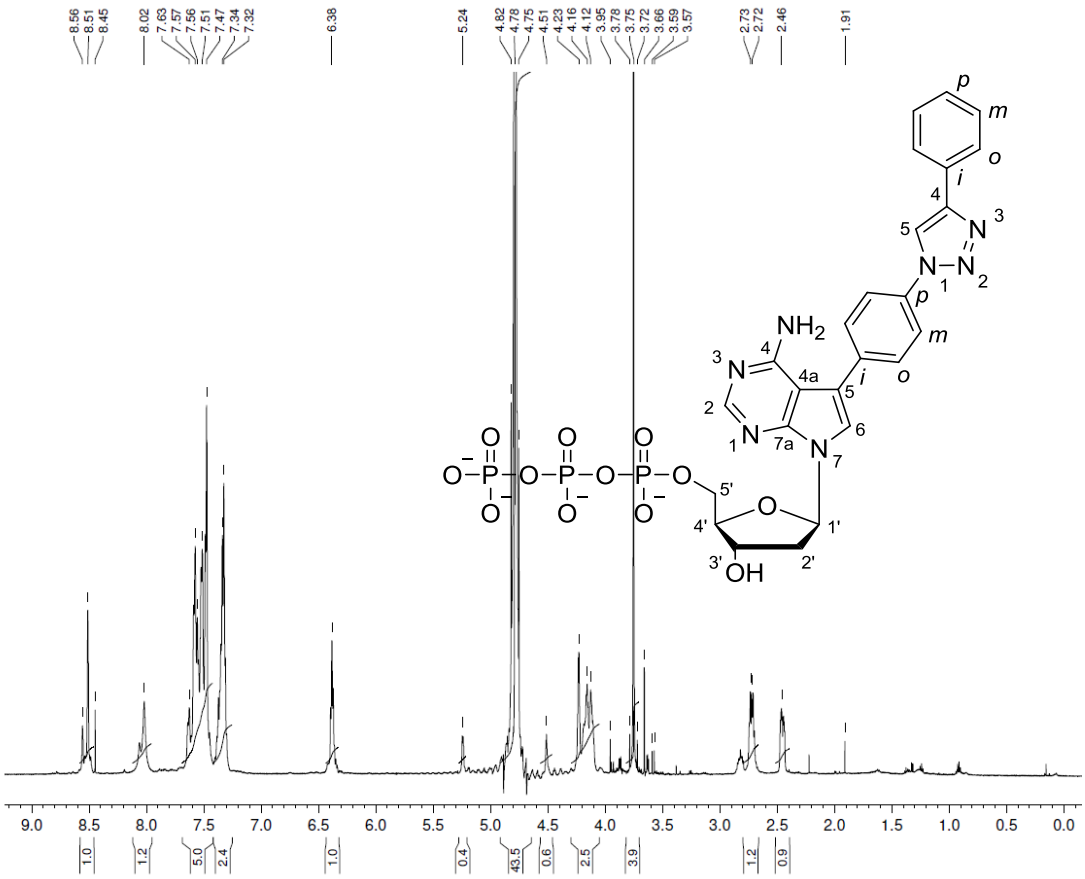

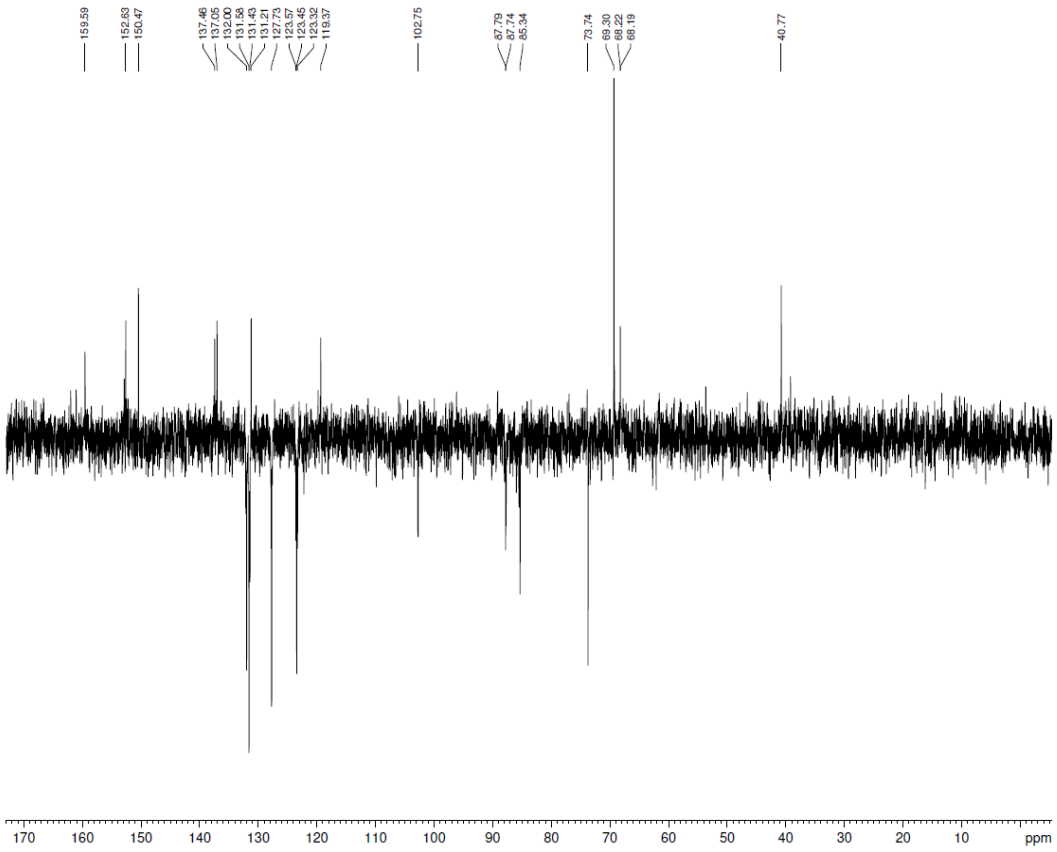
159.59
152.63
150.47
137.46
137.05
132.00
131.58
131.43
131.21
127.70
123.57
123.45
123.32
119.37
102.75
87.79
87.74
85.34
73.74
69.30
68.22
68.19
40.77
170 160 150 140 130 120 110 100 90 80 70 60 50 40 30 20 10 ppm

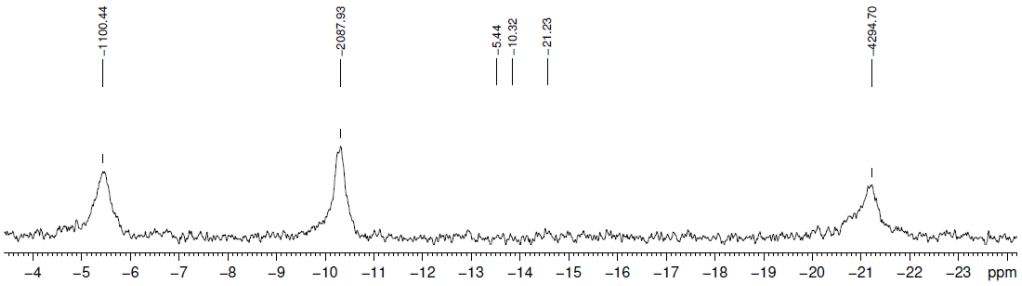
-1100.44
-2087.93
-5.44
-10.32
-21.23
-4294.70
−4 −5 −6 −7 −8 −9 −10 −11 −12 −13 −14 −15 −16 −17 −18 −19 −20 −21 −22 −23 ppm

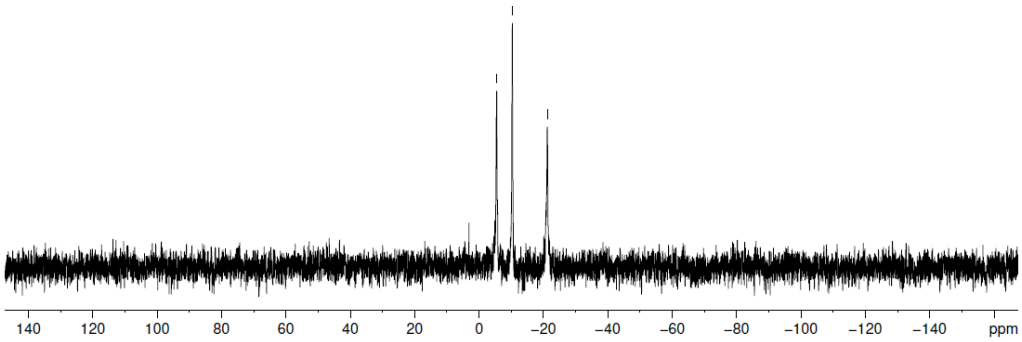
140 120 100 80 60 40 20 0 −20 −40 −60 −80 −100 −120 −140 ppm

$^{1}$H NMR, $^{13}$C and $^{31}$P spectra of **dC$^{TNO2}$TP.**

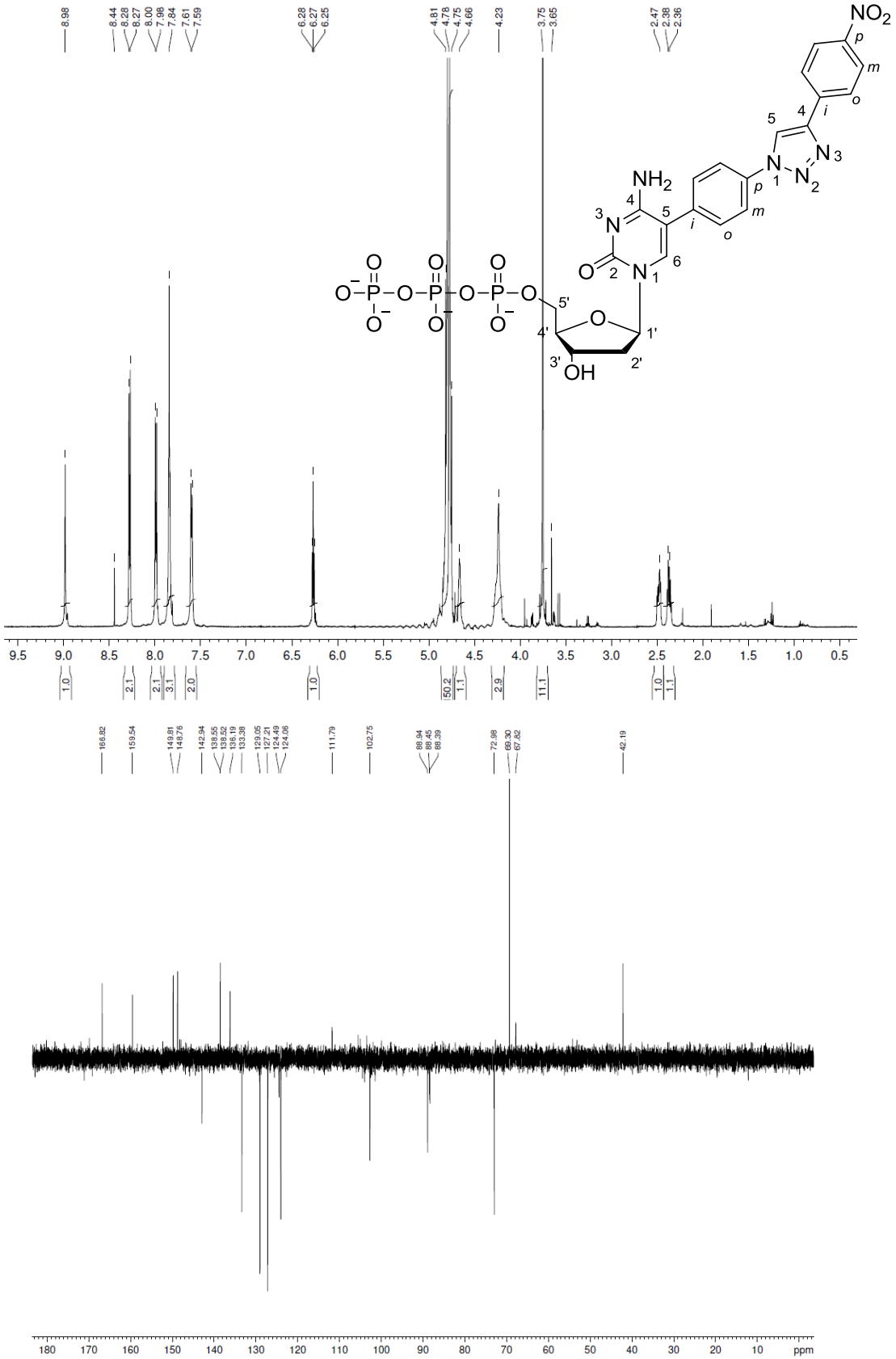

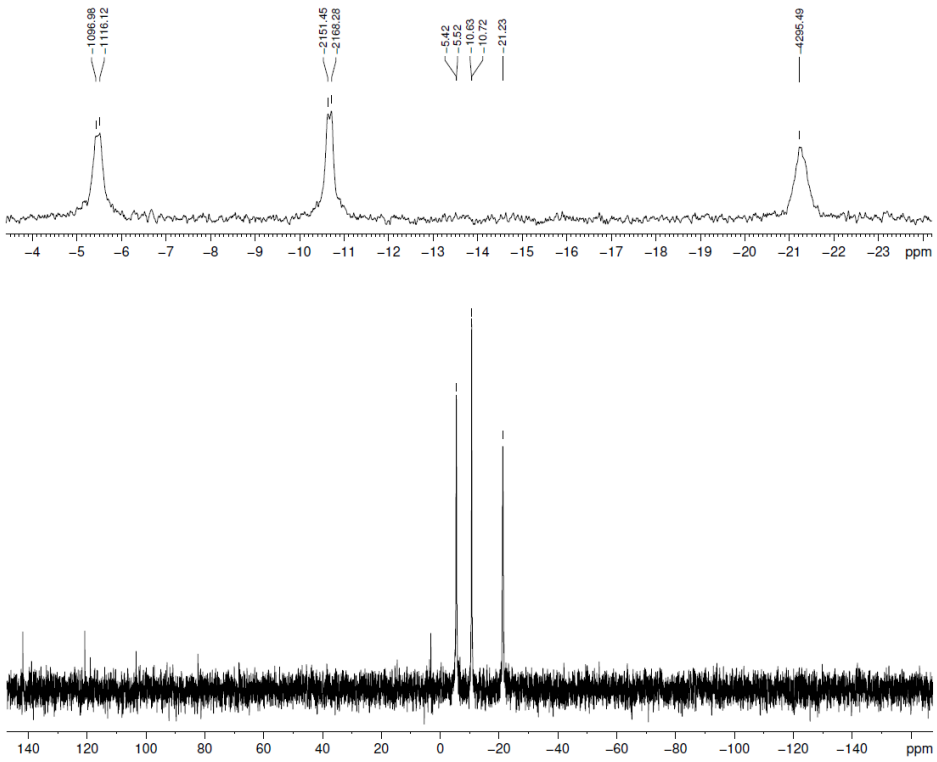


$^{1}$H NMR, $^{13}$C and $^{31}$P spectra of **dA$^{TNO2}$TP.**

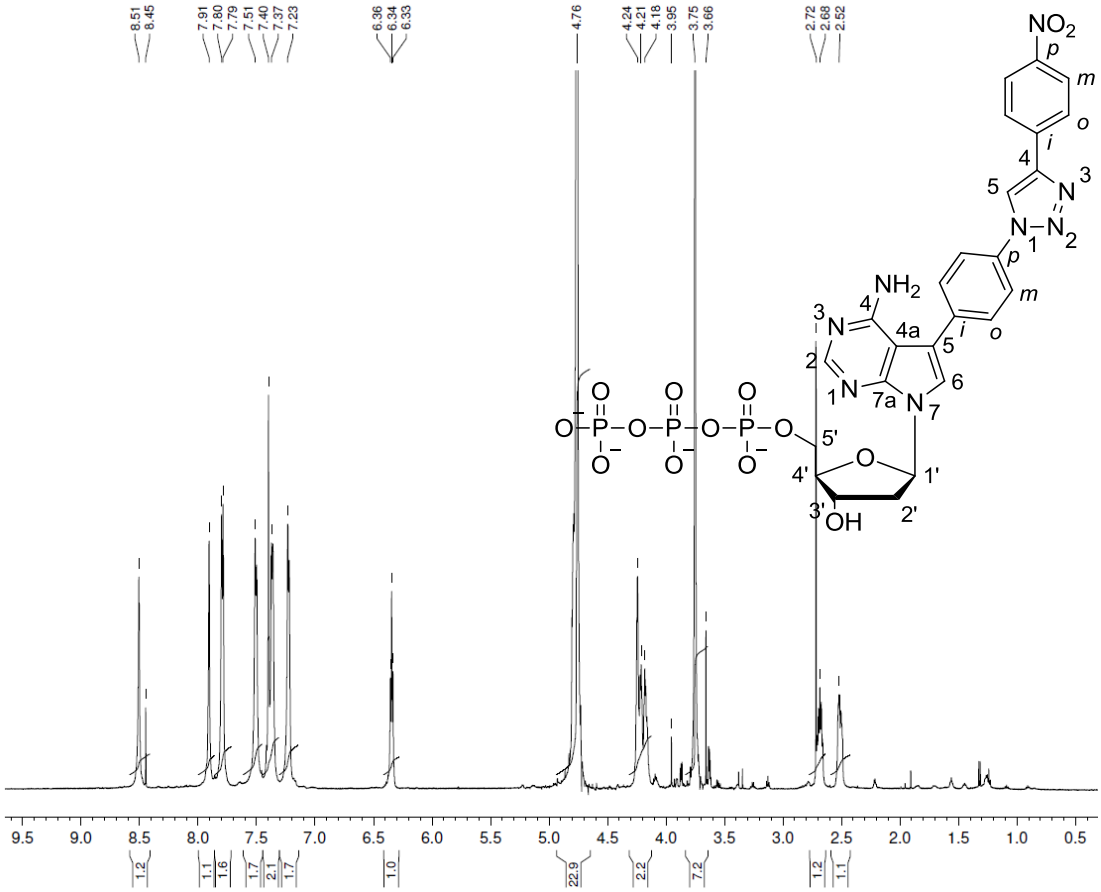

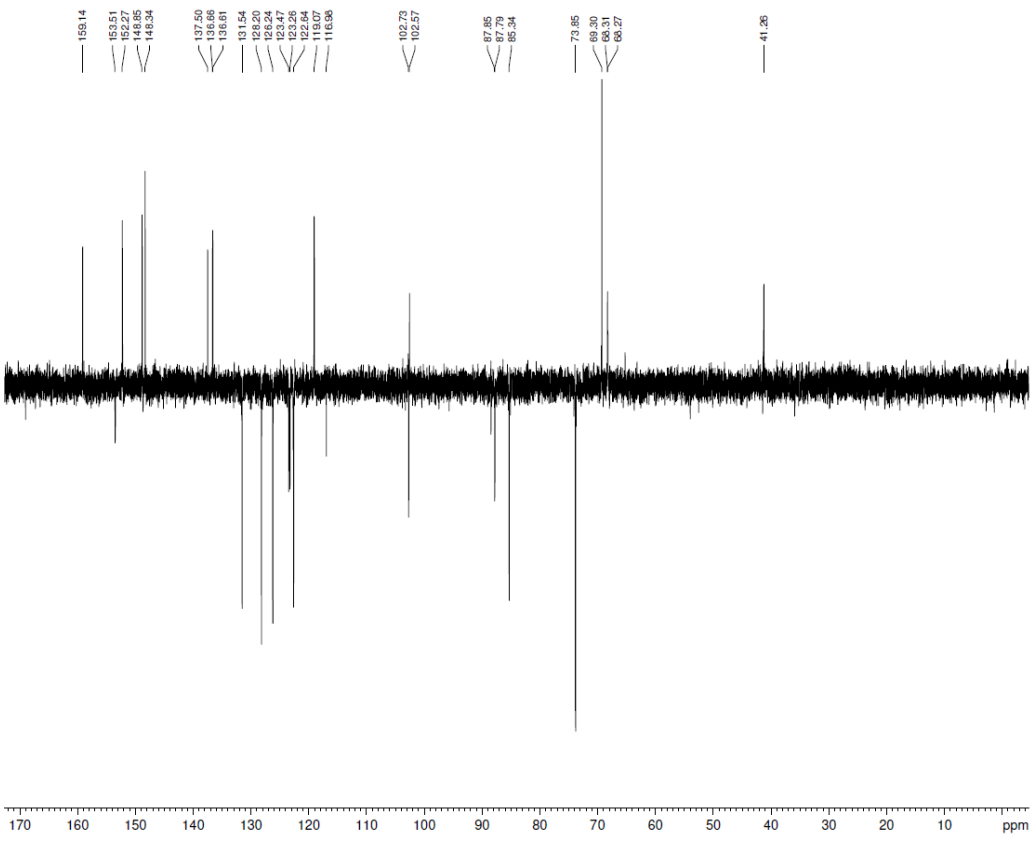
159.14
153.51
152.27
149.85
148.34
137.50
136.66
136.61
131.54
128.20
126.24
123.47
123.26
122.64
119.07
116.96
102.73
102.57
87.85
87.79
85.34
73.85
69.30
68.31
68.27
41.26
170 160 150 140 130 120 110 100 90 80 70 60 50 40 30 20 10 ppm

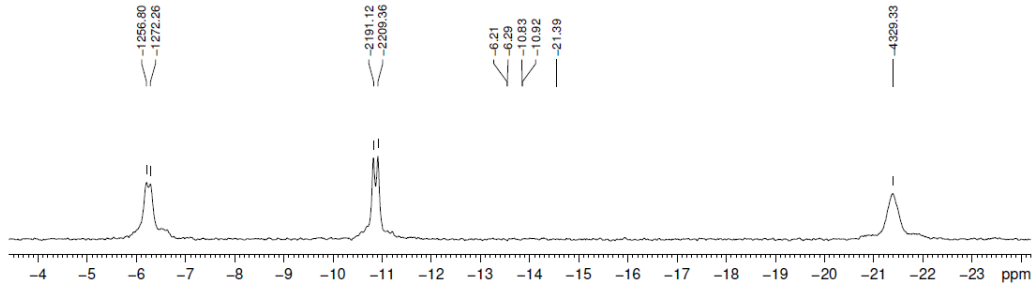
-1256.80
-1272.26
-2191.12
-2209.36
-6.21
-6.29
-10.83
-10.92
-21.39
-4329.33
−4 −5 −6 −7 −8 −9 −10 −11 −12 −13 −14 −15 −16 −17 −18 −19 −20 −21 −22 −23 ppm

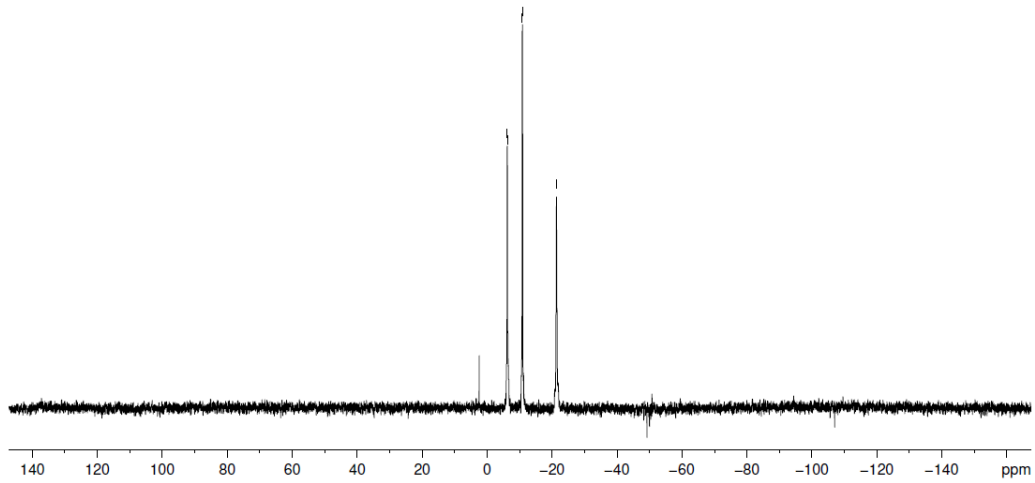
140 120 100 80 60 40 20 0 −20 −40 −60 −80 −100 −120 −140 ppm

# 9 Copies of Maldi-TOF spectra of DNA after click reaction

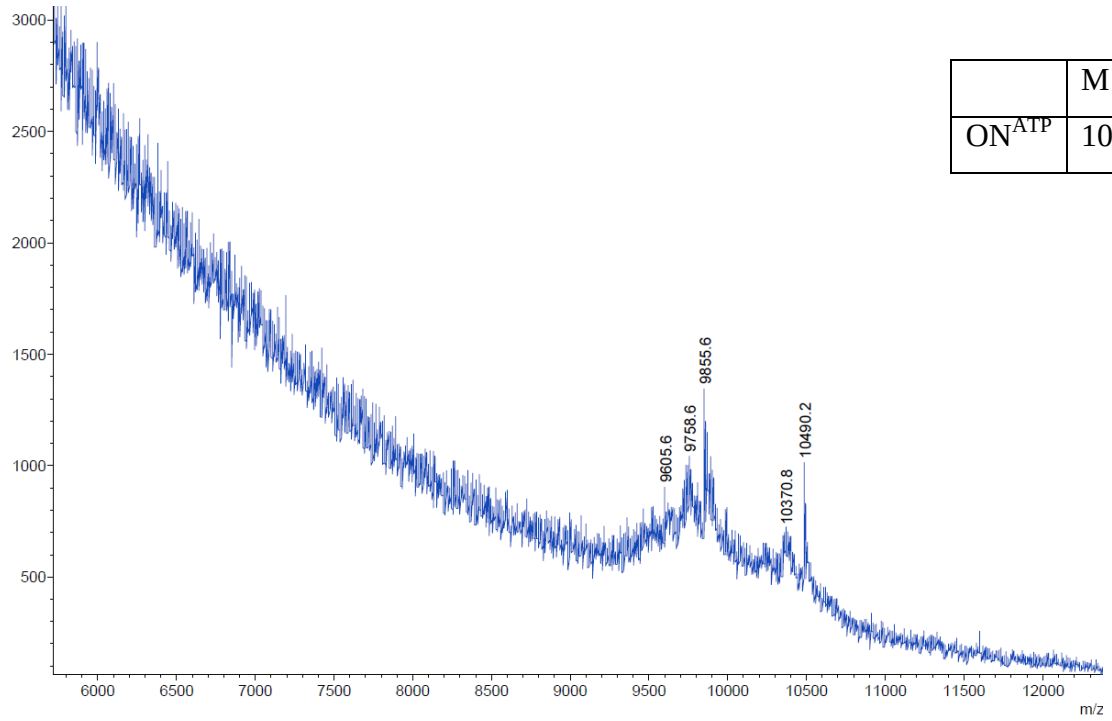


| | M [Da] |
|---|---|
| $ON^{ATP}$ | 10490.3 |

**Figure S21.** MALDI-TOF MS spectrum of $temp^{rnd16}$ with $A^{TP}$ modification (31 nt).

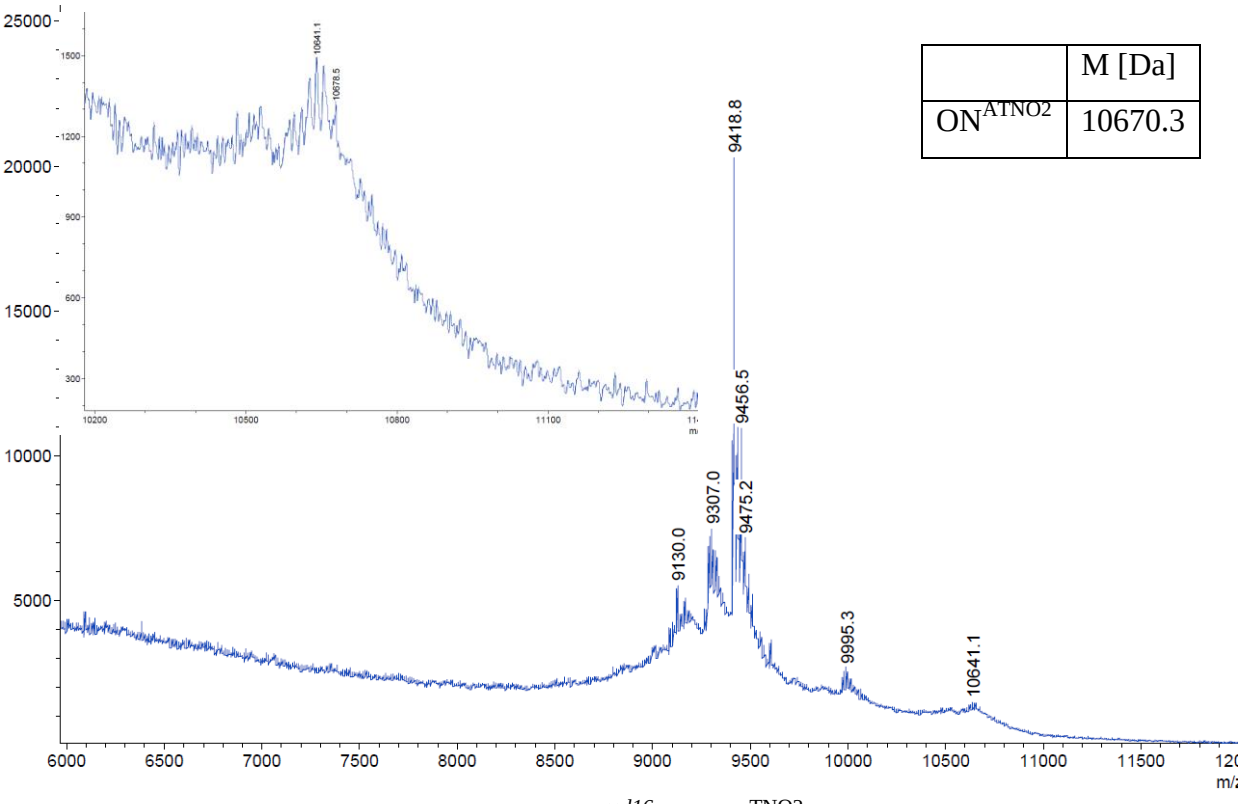


| | M [Da] |
|---|---|
| $ON^{ATNO2}$ | 10670.3 |

**Figure S22.** MALDI-TOF MS spectrum of $temp^{rnd16}$ with $A^{TNO2}$ modification (31 nt)

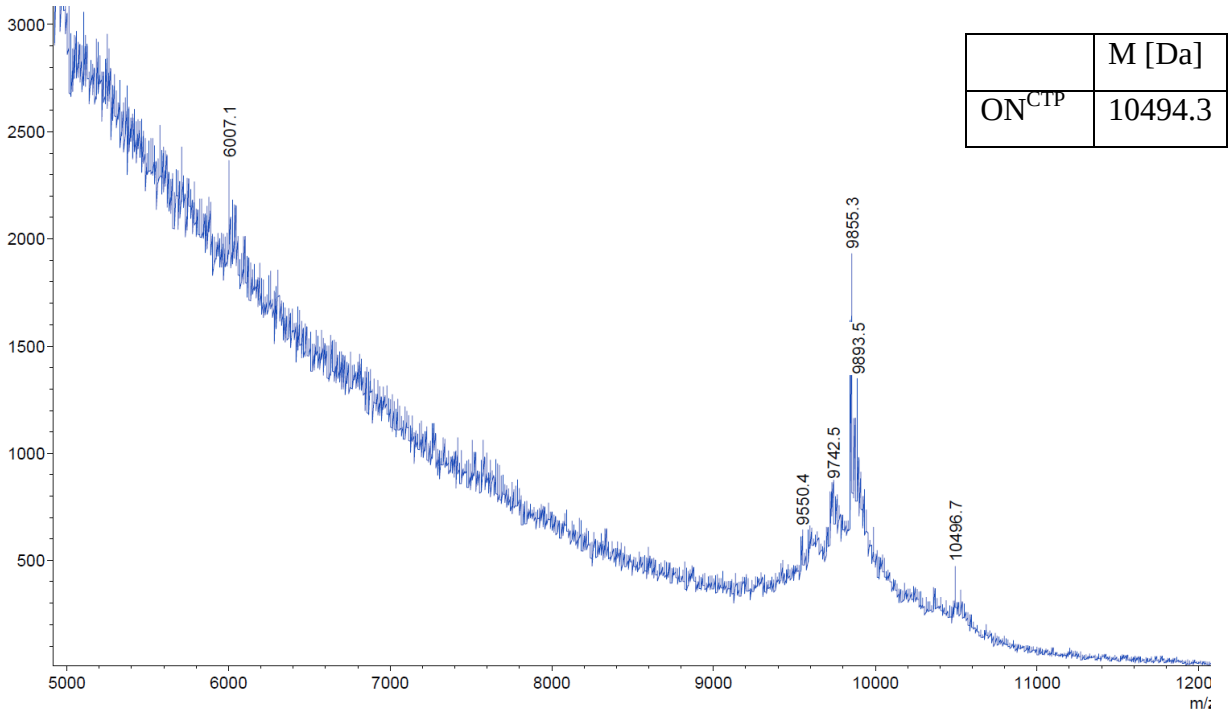


| | M [Da] |
|---|---|
| ON$^{CTP}$ | 10494.3 |

**Figure S23.** MALDI-TOF MS spectrum of temp$^{rnd16}$ with C$^{TP}$ modification (31 nt).

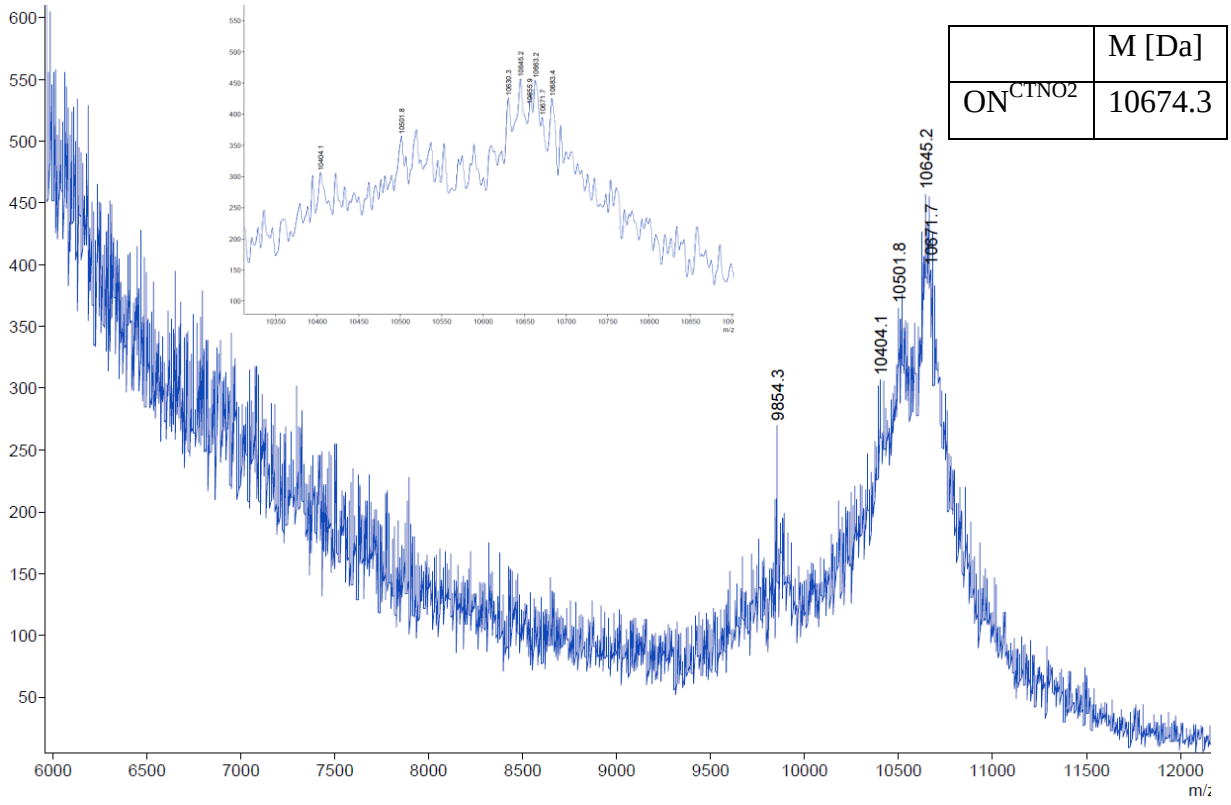


| | M [Da] |
|---|---|
| ON$^{CTNO2}$ | 10674.3 |

**Figure S24.** MALDI-TOF MS spectrum of temp$^{rnd16}$ with C$^{TNO2}$ modification (31 nt).

# 10 Copies of Maldi-TOF spectra

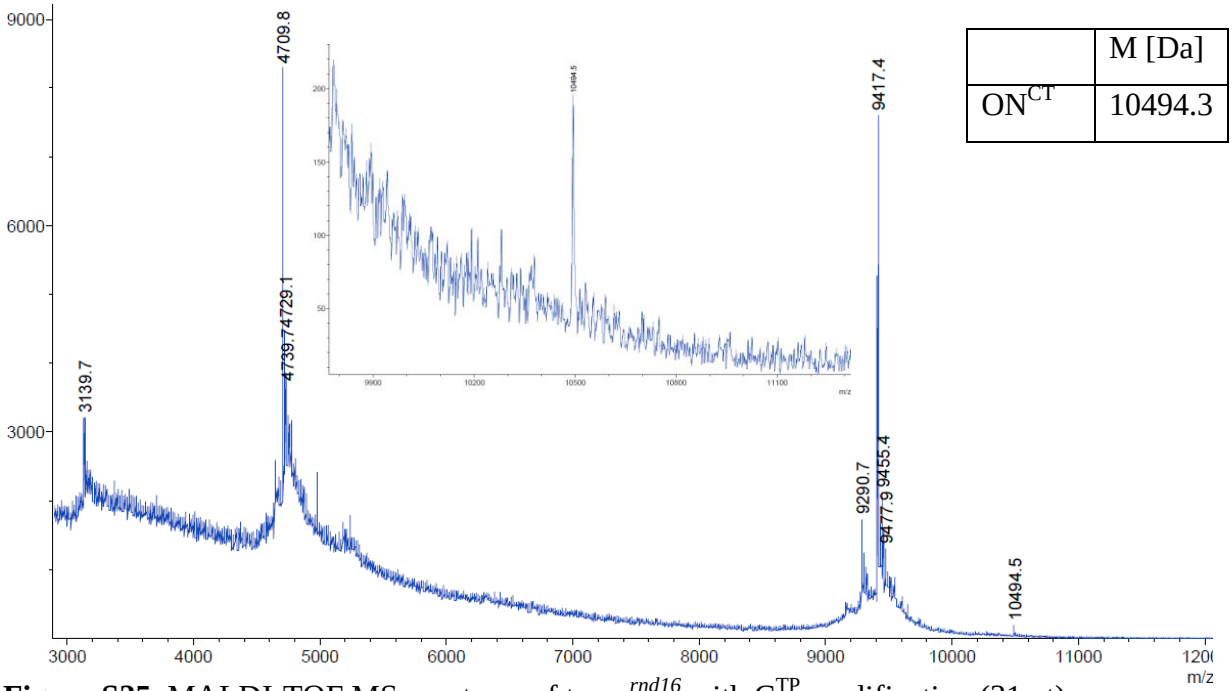


| | M [Da] |
|---|---|
| $ON^{CT}$ | 10494.3 |

**Figure S25.** MALDI-TOF MS spectrum of $temp^{rnd16}$ with $C^{TP}$ modification (31 nt)

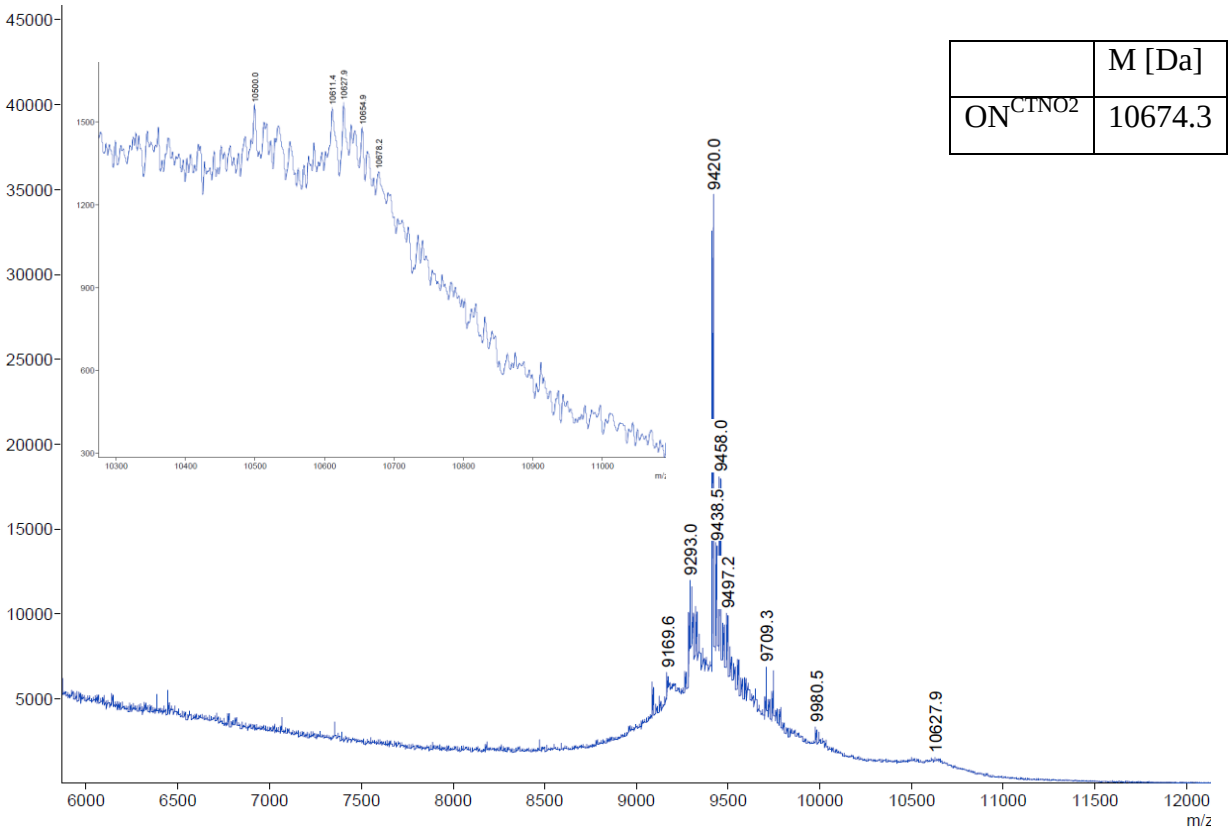


| | M [Da] |
|---|---|
| $ON^{CTNO2}$ | 10674.3 |

**Figure S26.** MALDI-TOF MS spectrum of $temp^{rnd16}$ with $C^{TNO2}$ modification (31 nt).

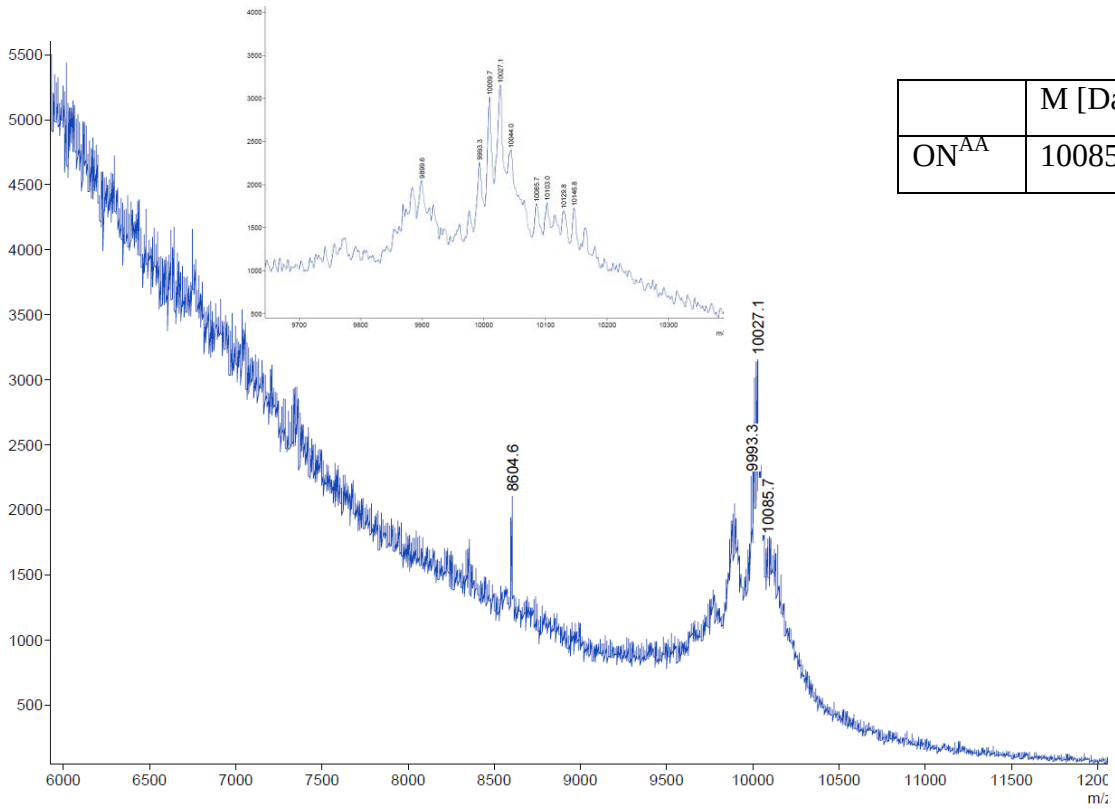


| | M [Da] |
|---|---|
| ON$^{AA}$ | 10085.8 |

**Figure S27.** MALDI-TOF MS spectrum of temp$^{rnd16}$ with A$^{A}$ modification (31 nt).

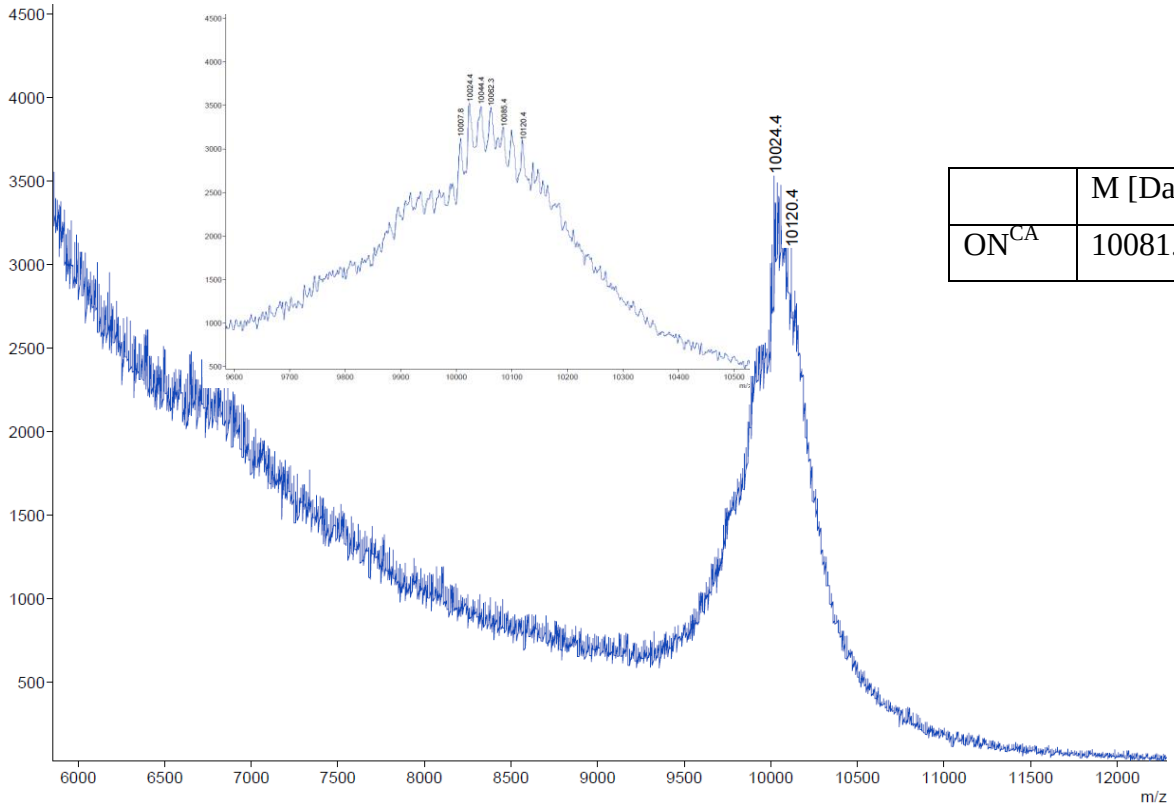


| | M [Da] |
|---|---|
| ON$^{CA}$ | 10081.8 |

**Figure S28.** MALDI-TOF MS spectrum of temp$^{rnd16}$ with C$^{A}$ modification (31 nt).